Joint ERCIM eMobility and MobiSense Workshop

Desislava Dimitrova, Marc Brogle,
Torsten Braun, Geert Heijenk
Nirvana Meratnia (Eds.)

Democritus University of Thrace
Petros M. Nomikos Conference Centre
Island of Santorini, Greece, June 8, 2012

Published: June 2012
University of Bern, Bern, Switzerland

ISBN 978-3-9522719-3-3

Preface

The sixth edition of the ERCIM eMobility workshop was held jointly with the second edition of the MobiSense workshop on the island of Santorini (Greece) on June 8, 2012. The joint workshop was hosted by the Democritus University of Thrace (Greece) in co-location with the 10th International Conference on Wired/Wireless Internet Communications. ERCIM, the European Research Consortium for Informatics and Mathematics, aims to foster collaborative work within the European research community and to increase co-operation with European industry. The ERCIM eMobility group dedicates its research to mobile applications and services that require technical solutions on various levels. In the ERCIM eMobility workshop current progress and future developments in the area of eMobility are discussed and the existing gap between theory and application closed.

The MobiSense workshop (Opportunistic Sensing and Processing in Mobile Wireless Sensor and Cellular Networks) is dedicated to the collaboration and interoperability among wireless sensor networks and other wireless networks, especially cellular ones. These border research topics are of interests due to their potential to enhance the performance of the currently deployed wireless technologies.

This year's edition of the workshops welcomed scientific research in the areas of cellular networks, intelligent transportation systems, novel routing solutions, inter-operability in heterogeneous networks and future interconnected network solutions. All papers have been carefully selected in a peer review process by the joint workshop technical program committee. In addition, an invited talk on Resilient Distributed Consensus was given by prof. Nitin Vaidya from the University of Illinois at Urbana-Champaign.

The joint workshop was held in the Petros M. Nomikos Conference Centre, located in the capital of Santorini, Fira. Fira (Thira) is the main of the five Santorini islands, a top world destination with its unique caldera, energy and beauty of the island.

We hope that all workshop delegates enjoyed the scientific program and discussion opportunities with colleagues. At this point, we wish to thank all authors of submitted papers and the members of the program committee for their contribution to the success of the event. The proceedings include work in progress papers as well as more in-depth full papers on the presented topics. We hope that workshop will continue to interest previous participants but will also interest new ones in the future as an event for the exchange of ideas and experiences.

Best wishes,
Mark Brogle and Desislava Dimitrova
TPC chairs

Torsten Braun, Geert Heijenk and Nirvana Meratnia
General chairs

General chairs

Torsten Braun, University of Bern, Switzerland
Geert Heijenk, University of Twente, The Netherlands
Nirvana Meratnia, University of Twente, The Netherlands

TPC chairs

Marc Brogle, Hewlett-Packard, Switzerland
Desislava Dimitrova, University of Bern, Switzerland

Technical program committee

Mari Carmen Aguayo-Torres, Universidad Malaga, Spain
Francisco Barcelo-Arroyo, UPC, Spain
Yolande Berbers, KU Leuven, Belgium
Robert Bestak, TU Prague, Czeck Republic
Thomas Michael Bohnert, ZHAW, Switzerland
Cristina Cano, Universidad Pompeu Fabra, Spain
Tao Chen, VTT Technical Research Centre, Finnland
Ozlem Durmaz-Incel, University of Bogazici, Turkey
Rossitza Goleva, Technical University Sofia, Bulgaria
Sonia Heemstra de Groot, TU Delft, The Netherlands
Jeung Hoyoung, SAP Research, Australia
Frank Legendre, ETHZ, Switzerland
Edmundo Monteiro, University of Coimbra, Portugal
Dritan Nace, UT de Compiegne, France
Gregory O'Hare, University College Dublin, Ireland
Hans Scholten, Universiteit Twente, The Netherlands
Vasilios Siris, ICS-FORTH / AUEB, Greece
Alexey Vinel, SPIIRAS, Russian Federation

Table of Contents

Part I

Invited Talk

Resilient Distributed Consensus

Nitin Vaidya

University of Illinois at Urbana-Champaign, Illinois, United States

Overview

Consensus algorithms allow a set of nodes to reach an agreement on a quantity of interest. For instance, a consensus algorithm may be used to allow a network of sensors to determine the average value of samples collected by the different sensors. Similarly, a consensus algorithm can also be used by the nodes to synchronize their clocks. Research on consensus algorithms has a long history, with contributions from different research communities, including distributed computing, control systems, and social science.

In this talk, we will discuss two resilient consensus algorithms that can perform correctly despite the following two types of adversities: (i) In wireless networks, transmissions are subject to transmission errors, resulting in packet losses. We will discuss how "average consensus" can be achieved over such lossy links, without explicitly making the links reliable, for instance, via retransmissions. (ii) In a distributed setting, some of the nodes in the network may fail or may be compromised. We will discuss a consensus algorithm that can tolerate "Byzantine" failures in partially connected networks.

Part II

Regular Papers

OptiPath: Optimal Route Selection Based on Location Data Collected from Smartphones

C. Kalampokis, D. Kalyvas, I. Latifis, and V.A. Siris

Mobile Multimedia Laboratory
Department of Informatics
Athens University of Economics and Business
vsiris@aueb.gr

Abstract. We present a system that selects the optimal route between two points for vehicles moving in an urban environment. Our approach uses location data gathered from smartphones, which includes route segments and their corresponding travel time. The system can be used as a standalone application with a user interface for path visualization. Additionally, route selection and location prediction can be used for improving streaming video applications and for scheduling delay tolerant data transfers to achieve mobile data offloading.

1. Introduction

Vehicular traffic congestion is a problem that concerns the inhabitants of urban areas. The problem of selecting travel paths that minimize the total travel time, thus accounting for congestion, has been investigated in the past, e.g. [1], while prior work has also investigated the use of wireless vehicular networks to gather information to select the best (shortest) route [2]. In this paper we present a client-server system (Fig. 1) for collecting real-time travel data over a cellular network from smartphones with geo-position sensors. This real-time travel data is used together with the list of possible routes from Google Maps, to select a route between an origin and a destination with the smallest travel time. The system consists of an Android client application called "OptiPath" and a multithreaded Java-based server with a database that contains the collected travel data.

The client, while in passive mode, records the route that is covered accompanied by real-time traffic information, such as speed and duration. The route consists of smaller segments that will be referred to as route tokens. Each route token contains the GPS coordinates of the route segment's start and end points, the speed, and the duration. Periodically, the route tokens are sent to the server using an Android service. The client's operation in passive mode operates as a seamless background process. The scalability of this approach is similar to that of other crowd-sourcing applications, e.g., to build a database with GPS and network bandwidth information [3].

In active mode, the user can use the client to select a desired destination, which together with his current location are placed in a query that is sent to the server, requesting the route between the two end-points with the shortest travel time. When the server receives a route query, it in turn sends Google Maps queries using the

Google Directions API[1], in order to obtain alternative routes between the two designated points. After it receives the alternative routes, the server computes the travel time for the alternative routes utilizing the relevant data stored in the database, and returns the route with the shortest travel time back to the OptiPath client. At the client, the server's response is graphically presented on a map.

2. System Operation

As we have outlined above, our architecture consists of two modes of operation, passive and active. Next we present in more detail the operation of each mode.

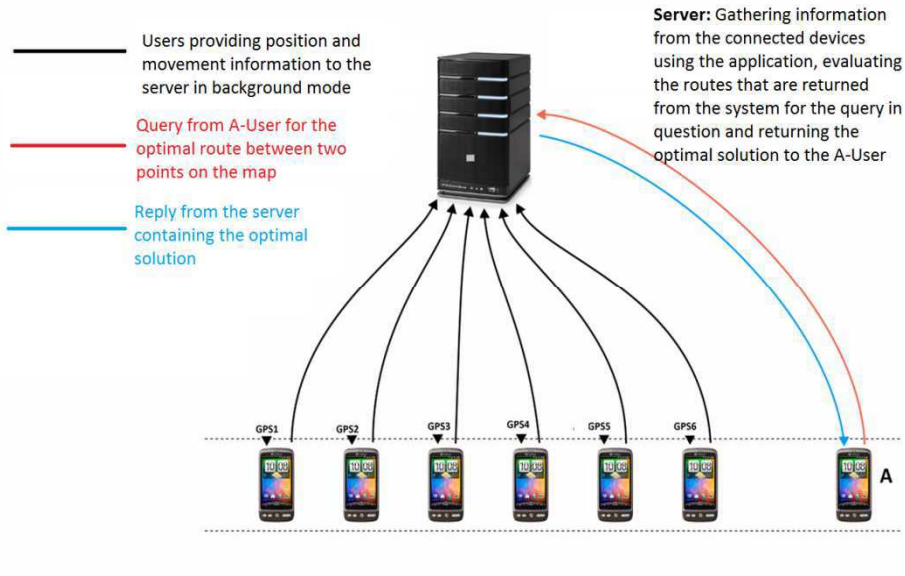

Fig. 1. Architecture and operation of OptiPath

Passive Mode:

On the client's side, OptiPath regularly creates route tokens by obtaining the GPS coordinates from the smartphone's sensor. After several experiments, we have concluded that the best accuracy is achieved when route tokens are created every ten meters. Such an interval provides sufficient accuracy when the vehicle turns at crossroads. Nevertheless, the interval's duration reflects a tradeoff between accuracy on one hand, and 3G bandwidth and mobile device processing power on the other hand. Creating tokens at fixed periods of time was rejected in order to avoid accepting zero-length tokens when the user remained stationary, e.g., during a traffic jam or

[1] Google Directions API Specification:
https://developers.google.com/maps/documentation/directions/

when the application is left running when not in use. Once several samples are collected, the application creates a list of tokens and sends it to the server, using a background Android Service. At the server's side, the route tokens received pass an integrity check and are inserted into the database.

Active Mode:

The user can choose a destination by touching a point on OptiPath's map or by searching an address using either the Google Places API[2] or the Google Places Autocomplete API[3]. The application creates a token that consists of the current location and the selected destination coordinates, which is forwarded to the server. When the server receives the token, it uses the coordinates of the starting and ending point, and creates a query to Google Maps for alternative routes between these two points. Google responds by sending one or more routes, consisting of tokens with different lengths compared to the tokens stored in database. Afterwards, the server creates a list of tokens for each alternative route. These lists are evaluated one by one using tokens stored in database according to the following procedure: Initially, the tokens from each route are mapped to possible matches contained in the database. The database tokens that are selected and eventually contribute to travel time estimation are those that overlap with the tokens from the proposed route either fully or partially. Note that the database tokens are usually shorter, since they are created every ten meters travelled distance. The matching procedure accounts for the possible lack of precision of the GPS signal by considering relaxed boundaries to determine the matching tokens. Specifically, the matching procedure involves checking if the database tokens are contained either fully or partially in the parallelogram that is created based on the Google route token with the corresponding error margins.

More recent tokens have a higher influence on the travel time estimates. Specifically, we group token samples based on when they were added into the database in three sets: route tokens added in the last 10 minutes, route tokens added 10-20 minutes ago, and route tokens added 20-30 minutes ago, which contribute to the travel time estimation with weight 60%, 25%, and 15%, respectively. We do not consider samples older than 30 minutes. If a token of the proposed Google route does not have a match in the database, then the precomputed Google estimation is considered in the travel time estimation.

After the above procedure, the optimal route with the shortest travel time, among the alternate routes provided by Google Maps, is returned to the client in a message that in addition to the estimated travel time also contains the total distance, the list of tokens, and the turn-by-turn directions, as provided by the Google Maps API. If the

---

[2] Google Places API Specification:
http://code.google.com/apis/maps/documentation/places/

[3] Google Places Autocomplete API Specification:
http://code.google.com/apis/maps/documentation/places/autocomplete.html

user deviates from the proposed route for some amount of time, then the application recommences the procedure, querying the server again for a new route and recalculating the optimal route from the current point to the initial destination, which it finally returns to the client.

3. Real world execution

To validate OptiPath we used two mobile devices with 3G connectivity, while the server was hosted on a remote computer. Two vehicles travelled along different routes. The testing location is shown in Fig. 2, where the two alternative routes A and B from the same start and end point are shown with different colours. The collection of tokens starts at Log point, hence Google Map's precomputed estimate is used as the travel time for the segment from the starting point to the log point.

Fig. 2. Two alternative routes between start and end points

We carried out two tests where the vehicles travelled from start to the end point several times. In the first test, vehicle 1 moved along route A (Fig. 3, left) with a higher average speed than vehicle 2, which moved along route B (Fig. 3, right). After completing the collection of tokens, the client sent a query for the optimal route between the start and end points. As a response to the query, route A was returned with score 180, against route B that had score 250; the score corresponds to the estimated travel time in seconds. In the second test, vehicle 1 moved along route A with a lower average speed than vehicle 2, which as before moved along route B. After completing the collection of tokens, the client created a query for the optimal route between starting and ending point. According to the response, route B was now evaluated with score 190, whereas route A received score 200.

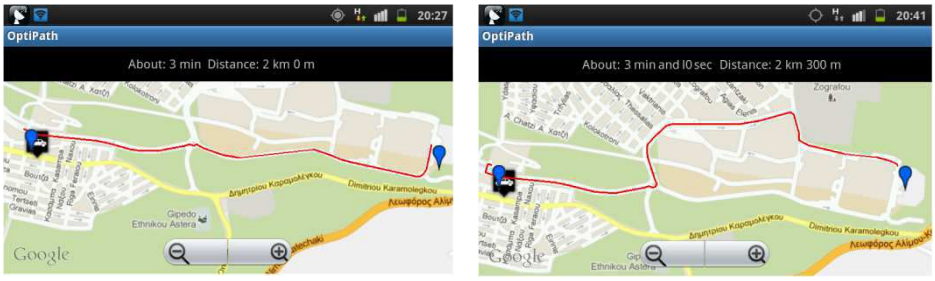

Fig. 3. Screen shots from the OptiPath client that depict the two alternate routes

4. Conclusion and Ongoing Work

We have presented the implementation of a system for determining the optimal route between two end-points based on the shortest travel time. The system utilizes data that includes route segments and their corresponding travel times, which are obtained from smartphones using crowd-sourcing.

Aside serving as a stand-alone application, the system's route selection and location prediction can be utilized for improving the performance of video streaming [3] and for scheduling delay tolerant data transfers to offload mobile traffic from cellular networks to WiFi hotspots [4]. These are directions we are currently investigating. In particular, the presented system can be enhanced or combined with a database containing the achievable throughput of a cellular network in different locations. This information combined with the prediction of the route and the position in different time instants allows planning of the transfer rate to avoid buffer under-runs, thus improving the performance of video streaming, while minimizing the maximum amount of buffer required [3]. Another direction involves the transmission of large files such as movies and pictures which are delay tolerant. This is becoming particularly popular with the increasing use of smartphones and mobile social networks, where users upload short clips or pictures in a delay tolerant manner. For such an application, estimates of both the cellular and the WiFi hotspot throughput in different locations are necessary. The goal would be to utilize as much as possible WiFi hotspot access along the selected route, thus minimizing the use of cellular networks, while satisfying a maximum delay threshold [4]. Another interesting direction is to utilize route and location prediction to perform pre-fetching or proactive caching [5,6], which can be used to increase the performance of video delivery in cellular networks [7], and reduce the peak load of mobile networks by offloading traffic to WiFi hotspots [8].

References

[1] James F. Campbell, "Selecting routes to minimize urban travel time," Transportation Research Part B: Methodological, Volume 26, Issue 4, August 1992, Pages 261–274.

[2] Kevin Collins and Gabriel-Miro Muntean, "An adaptive vehicle route management solution enabled by wireless vehicular networks," in Proc. of IEEE VTC 2008-Fall.

[3] H. Riiser, P. Vigmostad, C. Griwodz, and P. Halvorsen, "Bitrate and video quality planning for mobile streaming scenarios using a GPS-based bandwidth lookup service," in Proc. of ICME, 2011.

[4] A. Balasubramanian, R. Mahajan, and A. Venkataramani, "Augmenting mobile 3G using WiFi," in Proc. of ACM MobiSys Conference, 2010.

[5] P. Deshpande, A. Kashyap, C. Sung, and S.R. Das, "Predictive Methods for Improved Vehicular WiFi Access," in Proc. of ACM MobiSys 2009.

[6] V.A. Siris, X. Vasilakos, and G.C. Polyzos, "A Selective Neighbor Caching Approach for Supporting Mobility in Publish/Subscribe Networks," in Proc. of ERCIM Workshop on eMobility. Held in conjunction with WWIC 2011.

[7] N. Golrezaei et al, "FemtoCaching: Wireless Video Content Delivery through Distributed Caching Helpers," in Proc. of IEEE Infocom 2012.

[8] F. Malandrino et al, "Proactive Seeding for Information Cascadesin Cellular Networks," in Proc. of IEEE Infocom 2012.

DYMO Routing Protocol with Knowledge of Nodes' Position

Enrica Zola, Francisco Barcelo-Arroyo

Universitat Politècnica de Catalunya, c/ Jordi Girona 1-3, Mòdul C3
08034 Barcelona, Spain
{enrica, barcelo}@entel.upc.edu

Abstract. Knowledge of the physical location of the nodes can improve the efficiency of routing protocols in Mobile Ad-hoc Networks (MANETs). In the Beacon-Less Routing (BLR) algorithm, for instance, the source node broadcasts its data packets while the forwarding node is selected in a distributed manner among all its neighbouring nodes. We propose to apply the forwarding strategy of BLR to the route discovery process of Dynamic MANET On-demand (DYMO) routing protocol. Assuming that position information is available at transmitting nodes, route request (RREQ) packets will be broadcasted with such information. All receiving nodes will compute whether they are in the forwarding area and, if so, they will calculate a delay which will be applied to the next RREQ broadcast. The node with lower delay will resend the RREQ first, thus selecting, in a distributed manner, the best located node in the forwarding area. With this modification in the DYMO protocol, it is expected that the amount of RREQs circulating in the network will reduce, thus lessening the routing overhead and improving the overall throughput.

Keywords: MANET; routing protocol; DYMO; DFD; localization.

1 Introduction

The task of routing in Mobile Ad-hoc Networks (MANETs) has to be performed by the user nodes. These nodes are mobile and, sometimes, unreliable. Knowledge of the physical location of the nodes can improve the efficiency of routing. Many protocols have been proposed: some are intended to minimize the search space for route discovery towards the destination node [1]; others apply the source routing in order to establish the geographical path that a packet has to follow towards its destination [2]. Still, both approaches share the idea of flooding the route requests (RREQs) through the network in order to establish a path to destination before sending data to it. Other authors propose to flood data packets in the network, without the need for routing table set up and maintenance. In the Beacon-Less Routing Algorithm (BLR) [3], for instance, the source node broadcasts its data packets while the forwarding node is selected in a distributed manner among all its neighbouring nodes. The knowledge of nodes' positions is a requirement in the BLR approach. As a contention-based

scheme, BLR is characterized by larger transmission delays. On the other hand, beacon-based protocols periodically share location information among neighbouring nodes in order to maintain their routing tables. The time interval chosen in the algorithm for the flooding of the location information will determine higher accuracy (i.e., short time interval) at the cost of higher overhead. The Dynamic Route Maintenance (DRM) algorithm [4] aims at dynamically adjust a node's beacon interval based on the neighbouring mobility information (i.e., shorter intervals for higher mobility nodes), thus reducing the cost of route maintenance in low mobility scenarios while improving packet delivery rates in high mobility environments.

In this paper, we propose to apply the forwarding strategy of BLR to the route discovery process of Dynamic MANET On-demand (DYMO) routing protocol [5]. DYMO, also known as AODV2, is a reactive protocol in which a source node first establishes a route to a destination node before sending data to it. The main difference with AODV is that intermediate nodes learn the route to all the predecessor nodes in the path, thus lessening the number of RREQs generated in the network.

The main assumptions in our proposal are:

1. Nodes always know their own position (i.e., through GPS).
2. Nodes always know the destination node's position.

Destination node's position may be available at the source node through an external location management system, as commonly assumed in the literature [3, 6-8]. With this change in the DYMO protocol, we expect that the routing overhead will decrease. At each hop, fewer nodes will be contending the access for the rebroadcast of the RREQ, thus reducing the probability of collision. Despite the delay added to the retransmission of RREQ, we expect that, with fewer collisions in the network, the final delay of the route set-up will be almost the same, while the overall throughput will increase. Many proposals can be found that aims to improve the route discovery process by using location information of the nodes. Some authors propose that the RREQ is forwarded only by nodes in the *forwarding region* [9-10] or according to nodes' mobility information [11-12]. To the best of our knowledge, the approach described here, which has been proposed for flooding approaches, has never been applied to the route discovery process of AODV or DYMO protocols.

The remainder of this paper is organized as follows. Section 1 provides a brief introduction to routing protocols in MANETs. The proposed routing scheme is described in Section 2. Section 2.1 provides details on the modified route discovery process, while the algorithm for the selection of the forwarding node is described in Section 2.2. Section 3 concludes the paper.

2 Using Position Information in DYMO

The basic operations of the DYMO protocol [5] are route discovery and route management. Route discovery starts when a node (A) has to send data to another node (O) for which a route has not been established, yet. Source node A broadcasts a special message called Route Request. Every neighbour of A will hear the RREQ and

will add A as next hop in its routing table (i.e., direct transmission). Then, if this node knows how to reach O, it has to send a Route Reply (RREP) back to A; otherwise, it has to rebroadcast the RREQ. Before rebroadcast, it adds its address in the path accumulation field (i.e., RREQ in DYMO gets bigger as more hops are required to reach the destination). With path accumulation, any intermediate node learns its next hop towards A and towards all the predecessor nodes in the accumulated path. Once the RREQ has reached O or any node that is aware of how to reach O, a RREP is unicasted back to A, thus setting up the path (i.e., next hop) at all the intermediate nodes. In this paper, a modification in the route discovery process is proposed, assuming that each node knows its own position. Moreover, it is assumed that the source node knows the destination node's position. How the position information is available at the source node is out of the scope of this paper.
In Section 2.1, the modified algorithm for the route discovery in DYMO is described. Details on how to select the forwarding node (i.e., the one in charge of the RREQ retransmission) are provided in Section 2.2.

2.1 Modified Route Discovery

When a source node wants to send a packet to a given destination for which a route has not been established yet (i.e., no entry is found in its routing table), it will broadcast a RREQ packet, as defined by DYMO [5]. According to our proposal, the transmitter node's position (TX_pos) and the destination node's position (DST_pos) should be added in the RREQ. Any node in the proximity of the source node will receive the RREQ. If a node knows the route to destination, it will send a RREP immediately to the source node (same as in DYMO). In case no RREP has been heard, we propose that only the *best node* will rebroadcast the RREQ. The selection of the best node is explained in Section 2.2. With this modification, it is expected that the amount of RREQ circulating in the network will reduce if compared to DYMO, thus lessening the routing overhead. Before rebroadcast the RREQ, the best node will update the TX_pos field in the RREQ with its own position.
In DYMO and AODV, the number of RREQs for the same path is equal to the number of nodes (N) in the network, since every node that receives a RREQ is expected to rebroadcast it. In the proposed algorithm, the number of RREQs grows linearly with the number of hops between source and destination (*num_hops*). Despite the increase in the length of the RREQ due to the two added fields (TX_pos and DST_pos), the modification will significantly reduce the amount of routing overhead. In the worst-case scenario (see Section 2.2), three neighbours of the source node will rebroadcast its RREQ since they do not see each other (i.e., *hidden node problem*). This would cause, in the worst-case, a number of RREQ of $3 \cdot num\_hops$, which is always less than in the original DYMO algorithm.

2.2 Best Node's Selection

The selection of the best node (i.e., the intermediate node that is in charge of rebroadcast a RREQ first) is performed in a distributed manner. This behaviour has been taken from the BLR algorithm [3], where data packets are broadcasted through

the network, until they reach the destination. Routing tables are not used in BLR. The forwarding node is selected in a distributed fashion, by applying the shortest delay to the "best forwarding node": at each hop, the node with the best position in the forwarding area is selected to rebroadcast the data packet. The same idea is applied here to the broadcast of the RREQ.
Any node who has received a RREQ for which a route is still unknown will calculate (see Fig. 1):

1. The distance between the transmitter and the destination ($dist_{tx\_node}$). Recall that TX_pos and DST_pos are included in each RREQ.
2. Its distance to the destination (own_dist).
3. Its distance to the straight line that goes from the transmitter of the RREQ to the destination (height, *h*).

Only nodes with own_dist shorter than $dist_{tx\_node}$ are possible candidates for rebroadcast the RREQ. All the other nodes will throw the RREQ. Each candidate node will delay the rebroadcast of the RREQ according to the values previously calculated. This concept is known in the literature as Dynamic Forward Delay (DFD) [3]. The best node is the node with the lowest forward delay. The DFD is calculated as a function of the node's own_dist and height, in order to allow the node with the best position in the forwarding area to be the first that rebroadcasts the RREQ. The other candidate nodes that hear this RREQ will defer from rebroadcasting it again. In case multiple RREQs reach the destination node (i.e., due to the hidden node problem), the first RREQ received at destination node will be selected (i.e., the sequence number in the RREQ will preserve loops).
Let's consider the scenario in Fig. 1 to better explain the algorithm of the best node selection. In this example, source node A is looking for a path towards destination node O. Its RREQ is received by nodes B, C, D, E, F, and G (i.e., they lay inside the blue coverage area of A). The dashed line represents the points at $dist_{tx\_node}$ (i.e., $dist_{AO}$ in Fig. 1) which lay inside the coverage area of A. Nodes B, C, D, F are candidates for rebroadcast the RREQ since their distance to O is shorter than $dist_{tx\_node}$. Since D has the shortest own_dist and the shortest height among them, it will first rebroadcast the RREQ (i.e., D is the *best node* at this hop). All the other candidates are inside the coverage range of D, so they defer from rebroadcast the RREQ.

In the scenario depicted in Fig. 2, according to the geometry, up to three nodes will rebroadcast a RREQ (worst-case hidden node scenario). Nodes B, C and D do not hear each other, thus they all rebroadcast the RREQ. Of course, in dense scenarios like the one depicted here, the RREQ rebroadcasted by B will first reach the destination node O (i.e., since it has shorter own_dist and shorter height if compared with C and D, B will broadcast the RREQ first), thus guaranteeing the establishment of the shortest path even in this worst-case scenario.

Consider the case, in which two nodes have same own_dist, same height, and both are "best nodes". They will apply the same delay, so a collision may occur. If so, all the nodes in their collision domain will wait a backoff [13] and then delay again the retransmission according to the DFD. Further research is needed in order to evaluate the impact of collisions on the selection of the best route, since it is possible that the

backoff at the best node will defer its transmission more than at a node with worst position. Still, even when the optimal route is not selected due to collisions, the proposed modification guarantees that only one node retransmits the RREQ, which is the goal of the proposal.

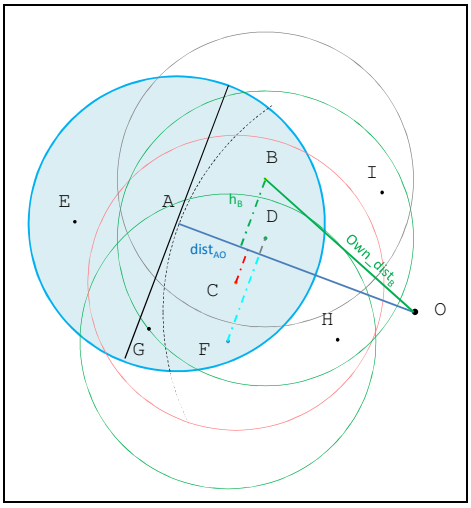

Fig. 1. *Best node* selection for rebroadcast the RREQ sent by A. D has the shortest own_dist and the shortest height.

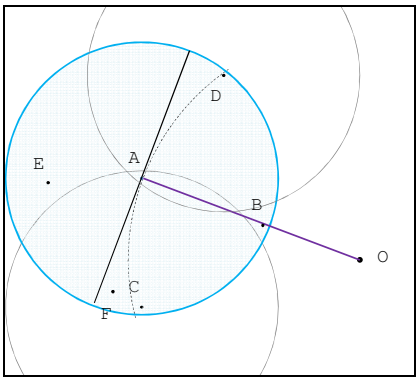

Fig. 2. Worst-case scenario: up to three nodes may rebroadcast the RREQ due to the hidden node problem.

The advantage that we expect from the application of the DFD to DYMO is two-fold. First, the routing overhead will decrease with respect to the original DYMO algorithm, even in the worst-case scenario. Second, if compared with DFD as used in BLR, the establishment of a route previous to sending data packets will guarantee higher throughputs, since confines broadcast to RREQ packets while data packets can be unicasted at higher rates (i.e., IEEE 802.11 nodes must use basic transmission rates for broadcasted frames [13]). Further investigation is certainly needed in order to prove this conjecture, but we expect strong improvements in the routing performance with this slight modification in the DYMO algorithm.

3 Conclusions

A modification in the route discovery process of the Dynamic MANET On-demand (DYMO) routing protocol is proposed here. The broadcast of the Route Request is delayed at each neighbour node as a function of its position in the forwarding area. In this way, the best located node will rebroadcast the RREQ first, thus preventing other nodes in its neighbourhood to also broadcast it. In order to calculate relative position in the forwarding area, each node should know its own position. Moreover, the source node should also know the position of the destination node. The position of the

transmitting node and of the destination node should be added to the RREQ. With these modifications in the DYMO protocol, it is expected that the amount of RREQ circulating in the network will reduce, thus lessening the routing overhead. With less control packets to send, collisions will also reduce thus improving the overall throughput in the network.

Acknowledgments

This work was supported by the Spanish Government and ERDF through CICYT project TEC2009-08198.

References

1. Ko, Y., Vaidya, N.H.: Location-Aided Routing (LAR) in mobile ad hoc networks, in: Proceedings of ACM MobiCom, pp.66—75, (1998).
2. Giruka, V., Singhal, M.: A self-healing on-demand geographic path routing protocol for mobile ad-hoc networks, Ad Hoc Networks, 5 (7), 1113-1128, (2007).
3. Heissenbüttel, M., Braun, T., Bernoulli, T., Wälchli, M.: BLR: Beacon-Less Routing Algorithm for Mobile Ad-Hoc Networks, Elsevier's Computer Communications Journal (Special Issue), 27, 1076-1086, (2003).
4. Chou, C.-H., Ssu, K.-F., & Jiau, H. C.: Dynamic route maintenance for geographic forwarding in mobile ad hoc networks, Computer Networks, 52(2), 418-431, (2008).
5. Perkins, C., Chakeres, I.: Dynamic MANET On-demand (AODVv2) Routing, IETF Internet Draft (Standards Tracks, work in progress), http://tools.ietf.org/html/draft-ietf-manet-dymo-22#page-33, (2012).
6. Endo, K., Inoue, Y., and Takahashi, Y.: Performance modeling of beaconless forwarding strategies in multi-hop wireless networks, Computer Communications, 35 (1), 120-128, (2012).
7. Li, J., and Mohapatra, P: LAKER: Location Aided Knowledge Extraction Routing for Mobile Ad Hoc Networks, in: Proc. IEEE Wireless Comm. and Networking Conf. (2003).
8. Blazevic, L., Le Boudec, J.-Y., Giordano, S.: A location-based routing method for mobile ad hoc networks, Mobile Computing, IEEE Transactions on, 4 (2), 97-110, (2005).
9. Patil, R., Damodaram, A., Das, R.: Cross layer AODV with Position based forwarding routing for mobile adhoc network, in: Wireless Communication and Sensor Networks (WCSN), 2009 Fifth IEEE Conference on, 1-6, (2009).
10. Reno Robert, R.: Enhanced AODV for directional flooding using coordinate system, in: Networking and Information Technology (ICNIT), 2010 International Conference on, 329-332, (2010).
11. Khamayseh, Y., Darwish, O.M., Wedian, S.A.: MA-AODV: Mobility Aware Routing Protocols for Mobile Ad Hoc Networks, in: Systems and Networks Communications, Fourth International Conference on, 25-29, (2009).
12. Dongxia, L., Xinan, F.: A revised AODV routing protocol based on the relative mobility of nodes, in: Wireless, Mobile and Multimedia Networks (ICWMNN 2010), IET 3rd International Conference on, 29-32, (2010).
13. "IEEE Std. 802.11-2012 Part 11: Wireless LAN Medium Access Control (MAC) and Physical Layer (PHY) specifications," IEEE Std. 802.11, (2012), http://standards.ieee.org/findstds/standard/802.11-2012.html.

Evaluating the Impact of Transmission Power on Selecting Tall Vehicles as Best Next Communication Hop

Yu Qiao, Wouter Klein Wolterink, Georgios Karagiannis, Geert Heijenk

University of Twente, the Netherlands

Abstract. The relatively low height of antennas on communicating vehicles in Vehicular Ad Hoc Networks (VANETs) makes one hop and as well multi-hop Vehicle-to-Vehicle (V2V) communication susceptible to obstruction by other vehicles on the road. When the transmitter or receiver (or both) is a Tall vehicle, (i.e., truck), the V2V communication suffer less from these obstructions. The transmission power control is an important feature in the design of (multi-hop) VANET communication algorithms. However, the benefits of choosing a Tall vehicle when transmission power is varied are not yet extensively researched. Therefore, the main contribution of this paper is to evaluate the impact of transmission power control on the improved V2V communication capabilities of tall vehicles. Based on simulations, it is shown that significant benefits are observed when a Tall vehicle is selected rather than a Short vehicle as a next V2V communication hop to relay packets. Moreover, the simulation experiments show that as the transmission power is increasing, the rate of Tall vehicles that are selected as best next V2V communication hop is significantly growing.

Keywords: VANET, V2V multi-hop communication, Tall vehicles, OMNET++ simulation

1 Introduction

Vehicular networking serves as one of the most important enabling technologies required to implement a myriad of applications related to vehicles, vehicle traffic, drivers, passengers and pedestrians. A Vehicular Ad-hoc Network (VANET) is a vehicular network that allows for Vehicle to Vehicle (V2V) communication. The proposed technology to perform this information exchange is the IEEE 802.11p technology [1], which is a member of the Wireless LAN family adapted for use in vehicular environments. A VANET enables a wide range of Intelligent Transportation System (ITS) applications, ranging from entertainment to traffic safety and efficiency, see e.g., [2]. Communication between vehicles can for example be used to realize driver support and active safety services like collision warning, up-to-date traffic and weather information, or active navigation systems.

The quality of communication between a sender and receiver in a VANET is determined by the quality of the received electromagnetic signal, and especially by the

strength of the signal. As a signal propagates from sender to receiver it is affected by obstacles in its path, such as surrounding buildings, foliage, but also other vehicles. In particular, the relatively low height of antennas on communicating vehicles in VANETs makes one hop and as well multi-hop V2V communication susceptible to obstruction by other vehicles on the road. When vehicles on the road communicate amongst themselves, other objects (e.g., buildings, other vehicles) could affect the wave propagation strongly. Existing research, see [3], [4], has shown that that other non-communicating vehicles often obstruct the line of sight (LOS) between the communicating vehicles, thus significantly decreasing their received power. In [4] the authors propose a propagation model that is able to model this effect. Furthermore, [4], [11] have shown how vehicles that have a greater height (i.e., trucks) suffer less from vehicle obstruction: when the transmitter or receiver (or both) is a Tall vehicle, the maximum distance over which communication is still possible is significantly larger than when neither the transmitter nor the receiver is a Tall vehicle. Tall vehicles can therefore better serve as next hop in multi-hop communication, because of their ability to communicate with nodes positioned further away. Choosing Tall vehicles as next hop may therefore significantly improve multi-hop communication algorithms.

However, a major limitation of the study presented in [4], [11] is related to the fact that only a limited number of parameters have been taken into account, and only a single scenario: the authors chose a single road topology in which they varied the ratio of Tall vehicles and the used transmission bit rate. Parameters that were not taken into account include the transmission power and traffic density. It is therefore unclear how this effect – the improved communication capabilities of Tall vehicles – is affected when the transmission power is varied.

Current VANET research is actively focusing on transmission power control as a means to create communication algorithms that are energy efficient, effective and scalable [5], [6]. In high traffic density situations these algorithms keep the transmission power low, in order to minimize the use of energy and to keep communication effective and scalable. As there is less traffic the transmission power can be increased, to ensure that a maximum amount of vehicles can reach each other. Transmission power control is currently being standardized by ETSI [7] and can be performed on a per-packet basis.

The transmission power control is an important feature in the design of (multi-hop) VANET communication algorithms. Furthermore, it is clear that the effect of choosing a Tall vehicle as a next hop can also significantly improve multi-hop V2V communication. However, the benefits of choosing a tall vehicle when transmission power is varied are not yet extensively researched. Therefore, the main contribution of this paper is to evaluate the impact of transmission power control on the improved V2V communication capabilities of Tall vehicles. Such V2V communication capabilities are the *Packet Success Rate (PSR)* and the *Rate of Tall vehicles selected as best next hop* to relay packets. *PSR* is defined as the ratio of the successful received beacons by all vehicles (under study), divided by the total number of beacons sent by all vehicles (under study), within a predefined transmission range. The research questions answered by this paper are:

- What is the impact of transmission power on the packet success rate in V2Vcommunications when different vehicle heights are used?
- How does the variation of the transmission power affect the effectiveness of choosing a Tall vehicle as a best next V2V communication hop?

The rest of the paper is organized as follows. Section 2 describes the simulation environment. The simulation experiments, the simulation results and their analysis are given in Section 3. The two research questions listed above are answered in Section 3. Finally, Section 4 concludes the paper and gives recommendations for future work.

2 Simulation Environment

For the simulations accomplished in this research work the OMNET++ network simulator v4.1 [8] combined with the MiXiM framework v2.1 [9] are used. To model the behavior of the IEEE 802.11p protocol as accurately as possible we have altered the IEEE 802.11 medium access module in such a way that all parameters follow the IEEE 802.11p specification [1]. In particular, the used carrier frequency is set to 5.9 GHz. In addition to the parameters used to emulate the IEEE 802.11p behavior, additional parameters are used, which are specified in Sections 3.2 and 3.3. More details on the used simulation environment can be found in [12].

2.1 Simulation Topology

The road topology used in this work is based on the parameters of Portuguese highway A28, which is a north-south motorway with length of 12.5km. The vehicle density on the road and the mix of Tall and Short vehicles are determined according to the Portuguese highway data set, see [4]. However, the two parameters can be varied in simulation to achieve different road traffic. In this paper, the vehicle density considered is 7.9 veh/km/lane. The mix of Tall and Short vehicles is: 15% Tall vehicles and 85% Short vehicles.

The topology used in the performed simulations is a 4-lane road, see Figure 1. Note that a bold black line in Figure 1 represents the center of a lane. The length of this road is 10km. The inter-lane distance is defined according to Trans-European North-South Motorway (TEM) Standards [10]. The used values are shown in Figure 1. In order to avoid border effects, the torus (set parameter 'useTorus' to true) topology is used in simulations, which means that the playground represents a torus with the borders (the begin and the end of axes) connected. Thus the distance between two hosts on the torus cannot be greater than 5km.

The vehicles are placed on the road based on:

- *number of vehicles on the road*: depends on the vehicle density
- *inter-vehicle spacing*: the distance between two adjacent vehicles moving on the same lane, see Figure 1. It is defined using an exponential distribution, see [4], [12]

- *type of vehicles*: two types of vehicles are distinguished, Tall, and Short vehicles, see [4], [12]
- *dimensions of vehicles*: this represents the length, width and height of both Tall and Short vehicles, see Table 1. These dimensions are random variables, but their values are set before placing the vehicles on the road.

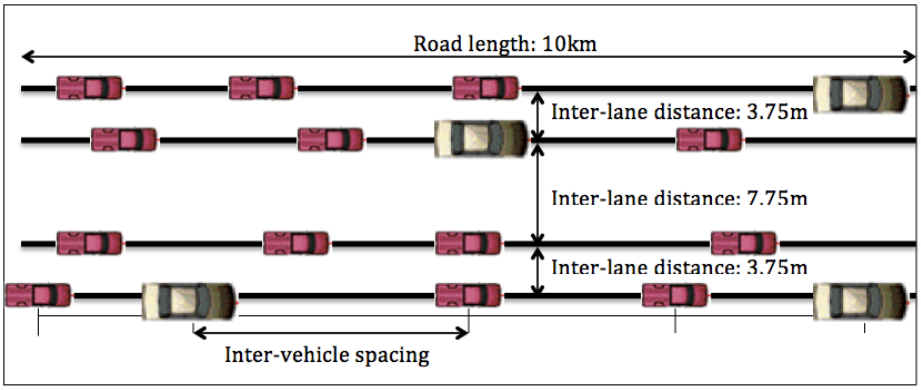

Fig. 1. Simulation topology

The vehicles are carrying transmitter/receiver antennas on their roofs, see [4]. In particular, each Short vehicle is carrying one antenna that is located on top of the vehicle and in the middle of the roof. Each Tall vehicle is carrying two antennas on the roof, one in the front and another in the back of the vehicle, see [11]. The height of each antenna is set to 10 cm and the antenna gain is set to 3dBi.

Table 1. Vehicle dimensions

Type	Parameters	Estimate
Short	Width	Mean: 175cm; Std. deviation: 8.3cm
	Height	Mean: 150cm; Std. deviation: 8.4cm
	Length	Mean: 500cm; Std. deviation: 100cm
Tall	Width	Mean: 250cm
	Height	Mean: 335cm; Std. deviation: 8.4cm
	Length	Mean: 1300cm; Std. deviation: 350cm

After the vehicles are placed on the road, simulation experiments are run in the following way. During one simulation run all the vehicles placed on the road will be transmitting in a sequential order at different (2 seconds) time intervals. This means that during a time interval of 2 seconds only one vehicle is transmitting one beacon with a length of 3200 bits. The other vehicles will successfully receive the beacon only if the power of the received signal is higher than a minimum receiver sensitivity threshold. The power of the received signal is measured at each receiving vehicle at the physical layer module incorporated in the OMNET++/MiXiM framework.

2.2 PROPAGATION MODEL

This section gives a brief description of the propagation model applied in this research.

Several propagation models applied in VANET research can be used to quantify the impact of vehicles as obstacles on the electromagnetic wave propagation. Since any channel model is a compromise between simplicity and accuracy, the target of this research is to construct a propagation model that is simple enough to be tractable from an implementation point of view, yet still able to emulate the essential V2V channel characteristics, mainly diffraction caused by mobile obstacles. A geometry-based deterministic model with computation reduction is suitable for the research presented in this paper. Geometry-based deterministic models, see e.g., [4], [13], [14], are based on a fixed geometry (sufficient information about environment and road traffic) and are used to analyze particular situations. The electromagnetic field arriving at receiver results from the combination of all components: direct component, reflected components, diffracted components and scattered components. Usually the ray-tracing method is used to analyze the characteristics of these components. A highly realistic model, based on optical ray tracing was proposed in [13]. The model is compared against experimental measurements and showed a close agreement. However, the accuracy of the model is achieved at the expense of high computational complexity and location-specific modeling. There are simplified geometry-based deterministic models, see e.g., [4][14]. In particular, the research work proposed by Boban et al. in [4] derive a simplified geometry-based deterministic propagation model, in which the effect of vehicles as obstacles on signal/wave propagation is isolated and quantified while the effect of other static obstacles (i.e., buildings, overpasses, etc.) is not considered. The research work in [4] focuses on vehicles as obstacles by systematically quantifying their impact on LOS and consequently on the received signal power. Although the propagation model calculates attenuation due to vehicles for each communicating pair separately, it is still computationally efficient. Based on these facts, i.e., realistic features, reduced computation, and concentration on mobile obstacles, we decided to enhance, implement and use the propagation model proposed in [4]. For the received power level, the impact of obstacles can be represented by signal attenuation. The attenuation on a radio link increases if one or more vehicles intersect the Fresnel ellipsoid corresponding to 60% of the radius of the first Fresnel zone, independent of their positions on the transmitter-receiver (Tx-Rx) link. This increase in attenuation is due to the diffraction of the electromagnetic waves. To model vehicles obstructing the LOS, we use the knife-edge attenuation model, see [15].

When there are no vehicles obstructing the LOS between Tx and Rx, we use the free space path loss model, see e.g., [16]. If only one obstacle is located between Tx and Rx, then the single knife-edge model described in ITU-R recommendation [15] is used. For the case that more than one vehicles (i.e., more than one obstacles) are located between Tx and Rx, the multiple knife-edge model with the cascaded cylinder method, proposed in [15], is used.

The knife-edge model described in [15] applies when the wavelength is fairly small in relation to the size of the obstacles, i.e., mainly to VHF and shorter waves (f > 30 MHz). Since the frequency of DSRC radios is 5.9 GHz the wavelength is approximately 5 cm, which is significantly smaller than the size of vehicles.

The propagation model is implemented in the OMNET++/Mixim framework.

3 Experiment Results and Analysis

Two sets of experiments are performed using the static parameters described in Section 2, such as road information, dimension of vehicles, antenna height, vehicle density and percentage of Tall vehicles. The first set of experiments answers the first research question and it evaluates the impact of transmission power on the *packet success rate* in V2V communications when different vehicle heights are used. The second set of experiments answers the second research question and it evaluates how the variation of the transmission power does affect the effectiveness of choosing a tall vehicle as a best next V2V communication hop.

In order to guarantee a high statistical accuracy of the obtained results, multiple runs have been performed and double-sided 90% confidence intervals have been calculated. More specifically, up to 50 runs are performed for the first set of experiments, and up to 200 runs are performed for the second set of experiments. Several graphs are depicting in addition to the average values also the confidence intervals in the form of upper and lower bars around their associated average values. For all performed experiments, the calculated confidence intervals are lower than the ±5 % of the shown calculated mean values.

3.1 Performance Metrics

Two performance metrics are defined and used in this paper.

3.1.1 Packet Success Rate (PSR)

The *Packet Success Rate (PSR)* is defined as the ratio of the successful received beacons by all vehicles (under study), divided by the total number of beacons sent by all vehicles (under study), within a predefined transmission range. A transmission range is defined by the radio coverage area of a transmitter.

A beacon is successfully received if the received power is higher than a minimum sensitivity threshold. The minimum receiver sensitivity threshold used in this research is -85dBm (data rate: 3Mbps, modulation: BPSK), see [17].

3.1.2 Rate of Tall vehicles selected as best next hop

In multi-hop routing it is usually desirable to cover a communication distance in as little hops as possible. This can be done by consistently having nodes select that neighbor node as a next hop that adds the largest number of second hop neighbors.

The best next hop in this paper is therefore defined as the one-hop neighbor that adds the largest number of second hop neighbors to the vehicle under consideration.

The *Rate of Tall vehicles selected as best next hop* is defined as the ratio of the total number of Tall vehicles in the system, selected as best next hop to relay packets, divided by the total number of vehicles in the system.

This performance metric is calculated based on the steps defined in [11]:

- With a certain percentage of Tall vehicle and a certain density, for each vehicle on the road, we find the farthest neighbouring Tall and farthest neighbouring Short vehicle that receives a packet correctly
- Next, we determine which of the two has the largest number of new neighbours (i.e., which adds the largest number of second hop neighbours to the vehicle under consideration)
- Finally, if the largest number of new neighbours is gained by using a Tall vehicle, we select it; otherwise, we select the Short vehicle as the best next hop.

3.2 Evaluation of the Impact of Transmission Power on the Packet Success Rate (PSR)

This section describes the first set of experiments and answers the first research question. The goal of this set of experiments is to evaluate the impact of the transmission power on the *Packet Success Rate (PSR)* in V2V communications when different vehicle heights are used. The parameters used during this set of experiments are given in Table 2.

In this set of experiments four types of transmission/reception (Tx/Rx) links are applied: (1) Tx and Rx are both Short vehicles (Short-Short), (2) Tx and Rx are Tall vehicles (Tall-Tall), (3) Tx is a Short vehicle while Rx is a Tall vehicle (Short-Tall) and (4) Tx is a Tall vehicle while Rx is a Short vehicle (Tall-Short).

Table 2. Parameters used in first set of experiments

Density	7.9 veh/km/lane
Spacing Mean	125m
Tx Power	{10, 18, 25, 33}dBm ({10, 63, 316, 1996}mW)
Ratio of Tall Vehicle	0.15 (15% Tall vehicles in the network)
Receiver Sensitivity threshold	-85 dBm (3 Mbps, BPSK)

Figure 2 shows the *PSR* results versus the transmission power for the 4 types of transmission/reception (Tx/Rx) links. From this set of experiments it can be concluded that:

1. all the *PSR* values associated with the Tall-Tall transmission/reception links are higher than all the *PSR* values associated with all other transmission/reception links

2. all the *PSR* values associated with the Short-Short transmission/reception links are lower than all the *PSR* values associated with all other transmission/reception links
3. all the *PSR* values associated with the Tall-Short transmission/reception links are higher than all the *PSR* values associated with the Short-Tall transmission/reception links
4. when the transmission power is increased the *PSR* average values for all types of transmission/reception links (i.e., Short-Short, Short-Tall, Tall-Short and Tall-Tall) are increasing
5. for the same transmission power and when the transmission range is increased then the average values of the *PSR* for all types of transmission/reception links are decreasing
6. as the transmission range is increasing, (i.e., 200m, 400m, 600m, 800m) the differences between the *PSR* average values associated with each of the transmission/reception links become larger when the transmission power is increased.

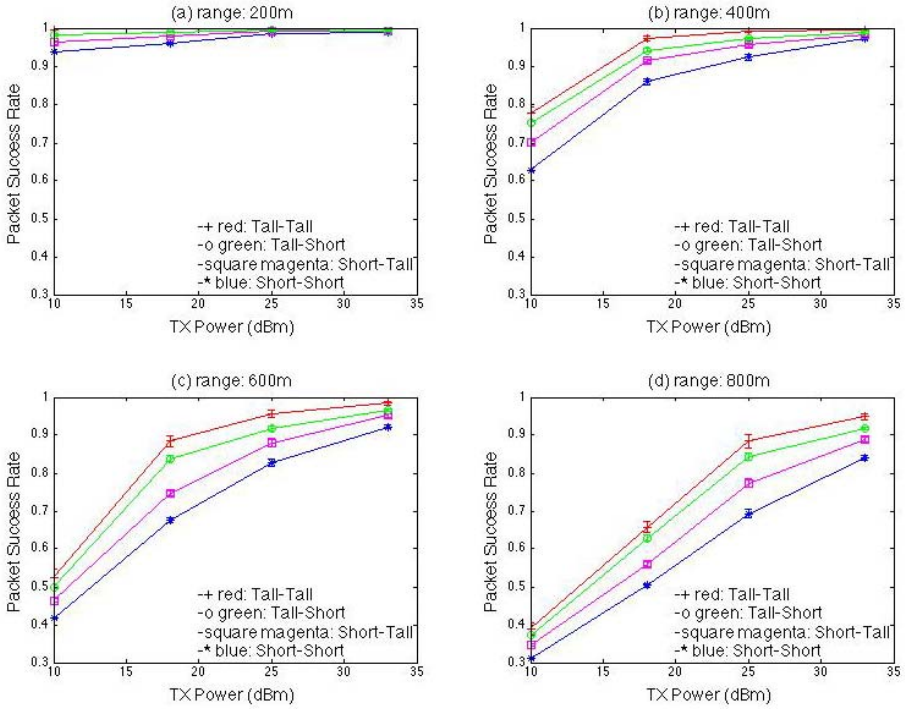

Fig. 2. *Packet Success Rate* (*PSR*) versus Transmission Power, for different transmission ranges (**a**): 200m, (**b**): 400m, (**c**): 600m, (**d**): 800m

3.3 Evaluation of the Impact of Transmission Power on Selecting Tall Vehicles as Best Next Hop

This section describes the second set of experiments and answers the second research question. The goal of this set of experiments is to evaluate how the variation of the transmission power does affect the effectiveness of choosing a tall vehicle as a best next V2V communication hop. The performance metric used in this set of experiments is the *Rate of Tall vehicles selected as best next hop*, see Section 3.1.2. The parameters used during this set of experiments are given in Table 3.

Table 3. Parameters used in second set of experiments

Density	7.9 veh/km/lane
Spacing Mean	125m
Tx Power	{10, 14, 18, 22, 25, 30, 33}dBm
Ratio of Tall Vehicle	{0.05, 0.10, 0.15, 0.20, 0.25, 0.30, 0.35, 0.40, 0.45, 0.5 }
Receiver Sensitivity threshold	-85 dBm (3Mbps, BPSK)

Figure 3 shows the *Rate of Tall vehicles selected as best next hop* results, when the transmission power and the ratio of Tall vehicles present on the road are varied.

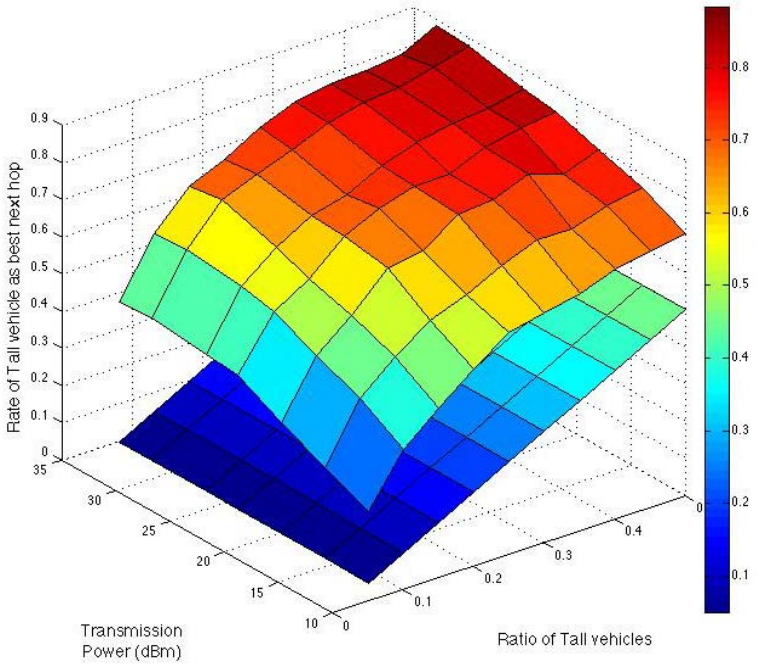

Fig. 3. *Rate of Tall vehicle as best next hop*, when varying transmission power and Ratio of Tall vehicles present on the road

The lower surface shown in Figure 3, represents a reference plane, where the value of the *Rate of Tall vehicles selected as best next hop* metric for each used transmission power is equal to the actual ratio of Tall vehicles present on the road. The upper surface represents the results of our simulation experiments. From this set of experiments it can be concluded that:

1. for all transmission power values and all ratios of Tall vehicles present on the road, the *Rate of Tall vehicles selected as best next hop* is higher than the ratio of Tall vehicles present on the road (the lower plane in Figure 3), which indicates that compared to Short vehicles, the Tall vehicles are better next V2V communication hops, regardless of the transmission power used.
2. as the transmission power increases, Tall vehicles become even better next V2V communication hops. The reason of this is that by increasing the transmission power, the maximum communication range increases and Tall vehicles have the ability to better exploit this large communication range as they have a larger probability of having a LOS with more vehicles that are located far away.

Note that additional simulation experiments have been performed and presented in [12], but due to page limitations these experiment results are not shown in this paper.

4 Conclusions and Future Work

In this article we evaluated the impact of transmission power control on the improved V2V communication capabilities of Tall vehicles. In particular, this paper evaluates (1) the impact of transmission power on the packet success rate in V2V communications when different vehicle heights are used and (2) how the variation of the transmission power does affect the effectiveness of choosing a tall vehicle as a best next V2V communication hop.

Based on simulations, it is shown that significant benefits are observed when Tall vehicles are selected rather than Short vehicle as a next communication hop to relay packets. Moreover, the simulation experiments show that as the transmission power is increasing the rate of Tall vehicles that are selected as best next V2V communication hop is significantly growing. In particular, the increase of this rate is amplified when in addition to the transmission power, also the ratio of Tall vehicles present on the road is increased.

Furthermore, based on the simulation experiments, we conclude that for realistic situations (i.e., inter-vehicle spacing mean: 125m, Tall vehicles percentage: 15%) the communication links that are using Tall vehicles as transmitter and/or receiver perform consistently and significantly better than the communication links that use Short vehicles, from the point of packet success rate. Moreover, when the transmission power is increased the packet success rate average values for all types of transmission/reception links (Short-Short, Short-Tall, Tall-Short and Tall-Tall) are increasing. However, for the same transmission power and when the transmission range is increased then the average values of the packet success rate for all types of communication links are decreasing. Furthermore, as the transmission range is increasing, the

differences between the packet success rate average values associated with each of the transmission/reception links become larger when the transmission power is increased.

As future work, we will use the model presented in this paper and focus on the investigation of VANET multi-hop and geo-cast communication algorithms and protocols, when (1) the effect of Tall vehicles on the V2V communication and (2) the benefit of choosing a Tall vehicle as a next hop are taken into account.

References

1. IEEE standard for information technology – telecommunications and information exchange between systems – local and metropolitan area networks – specific requirements part 11: wireless LAN medium access control (mac) and physical layer (phy) specifications amendment 6: wireless access in vehicular environments. 2010. IEEE Computer Society. IEEE P802.11p.
2. Karagiannis, G., Altintas, O., Ekici, E., Heijenk, G.J., Jarupan, B., Lin, K., Weil, T., Vehicular networking: A survey and tutorial on requirements, architectures, challenges, standards and solutions. IEEE Communications Surveys & Tutorials, vol. 13, nr. 4., pp. 584-616, 2011.
3. Meireles, R., Boban, M., Steenkiste, P., Tonguz, O., Barros, J., Experimental study on the impact of vehicular obstructions in vanets, Proc. of IEEE Vehicular Networking Conference (VNC), pp. 338-345, 2010.
4. Boban, M.; Vinhoza, T.T.V.; Ferreira, M.; Barros, J.; Tonguz, O.K.; Impact of Vehicles as Obstacles in Vehicular Ad Hoc Networks, Selected Areas in Communications, IEEE Journal on , vol.29, no.1, pp.15-28, January 2011.
5. Mittag, J., Eisenlohr, F.S., Killat, M., Härri, J., Hartenstein, H., Analysis and design of effective and low-overhead transmission power control for VANETs, Proc. of the 5th ACM international workshop on VehiculAr Inter-NETworking, 2008.
6. Torrent-Moreno, M., Mittag, J., Santi, P., and Hartenstein, H., Vehicle-to-Vehicle Communication: Fair Transmit Power Control for Safety-Critical Information, IEEE Transactions on Vehicular Technology, September 2009.
7. ETSI TS 102 687, Decentralized Congestion Control Mechanisms for Intelligent Transport Systems operating in the 5 GHz range, 2010.
8. OMNeT++ official website, to be found via (visited on April 2012): http://www.omnetpp.org.
9. MiXiM introduction in the sourceforge website, to be found via (visited on April 2012): http://mixim.sourceforge.net/.
10. TEM Project Central Office. Trans-European north-south motorway (TEM) standards and recommended practice. United Nations Economic Commission for Europe, 2002.
11. Boban, M., Meireles, R., Barros, J., Tonguz, O. and Steenkiste, P., Exploiting the height of vehicles in vehicular communication. IEEE Vehicular Networking Conference (VNC), 2011.
12. Qiao, Y., Karagiannis, G., Wolterink, W.K., Evaluating the Impact of Large Vehicles in Vehicular Communication, IP Research assignment, University of Twente, the Netherlands, March 2012, to be found via (visited on April 2012): http://www.utwente.nl/ewi/dacs/assignments/completed/bachelor/reports/2012-yuqiao.pdf.
13. Maurer, J., Fügen, T., Schäfer, T. and Wiesbeck, W., A new inter-vehicle communication (ivc) channel model. IEEE 60th Vehicular Technology Conference (VTC 2004-Fall), vol. 1, pp. 9-13, 2004.

14. Ledy, J., Boeglen, H., Poussard, A.M., Hilt, B. and Vauzelle, R., A semi-deterministic channel model for VANETs simulations. International Journal of Vehicular Technology, 2011.
15. ITU-R, Propagation by diffraction. International Telecommunication Union Radiocommunication Sector, Geneva, Recommendation P.526, 2007.
16. Rappaport, T. S., Wireless Communications: Principles and Practice. Prentice Hall, 1996.
17. Standard Specification for Telecommunications and Information Exchange Between Roadside and Vehicle Systems - 5GHz Band Dedicated Short Range Communications (DSRC) Medium Access Control (MAC) and Physical Layer (PHY) Specification, ASTM E2213-03, Sep. 2003.

Topology Control and Mobility Strategy for UAV Ad-hoc Networks: A Survey *

Zhongliang Zhao, Torsten Braun

Institute of Computer Science and Applied Mathematics, University of Bern
Neubrückstrasse 10, 3012 Bern, Switzerland
Email: {zhao, braun} @iam.unibe.ch

Abstract. Advances in electronics and software are allowing the rapid development of small unmanned aerial vehicles (UAVs), capable of performing autonomous coordinated actions. Developments in the area of lithium polymer batteries and carbon fiber-reinforce plastic materials let UAVs become an aerial platform, that can be equipped with a variety of sensors such as cameras. Furthermore, it is also possible to mount communication modules on the UAV platform in order to let the UAVs work as communication relays to build a wireless aerial backbone network. However, the cooperative operation between multiple autonomous unmanned aerial vehicles is usually constrained by sensor range, communication limits, and operational environments. Stable communication systems of networked UAVs and sensing nodes will be the key technologies for high-performance and remote operation in these applications. The topology of the UAV ad-hoc network plays an important role in the system performance. This paper discusses the state-of-art schemes that could be applied as the topology control of the UAV ad-hoc networks.

Keywords: UAVs, connectivity, coverage, mobility, topology control

1 Introduction

Recent developments of autonomous unmanned aerial vehicles (UAVs) and wireless sensor networks (WSNs) allow automated approaches to surveillance with minimal human intervention. A feasible solution is to deploy a set of UAVs, each mounted with a communication module like a wireless mesh node. In this way a wireless backbone can be built, over which various entities on the ground such as rescue teams, relief agencies, first responders can communication with each other. A system of aircrafts would provide mobile ad-hoc networks (MANETs) connecting ground devices with flying UAVs, as well as the inter-connection between different UAVs, as shown in Figure 1. One plausible approach to achieve this is to maintain a fully connected network of UAVs at all time, so that a given UAV can talk with any other UAVs using multi-hop ad hoc routing. However, oftentimes there are not enough UAVs to establish a continuous path between two points on the ground and this is a huge problem for solutions that require a fully connected UAV mesh. The notion of continuous path between end-points

* This work is partly supported by the Swiss National Science Foundation under grant number 200021-130211.

only makes sense when the relay nodes are stationary. When the nodes are capable of moving, especially in UAV ad-hoc networks that include nodes moving in a highly mobile way, it becomes extremely difficult to maintain continuous connectivity. Therefore, a decentralized agent-based motion planning approach is usually applied for UAV controlling. Compared with the centralized approach, autonomous agents are more robust against wireless link failures which might happen due to poor coverage and reliability of cellular technologies in higher altitudes. Since UAVs have to fly with a certain formation to keep connectivity with each other, topology control plays a crucial role. In this paper we give a review of existing typical swarm models proposed in the literature that could be applied for deploying and controlling groups of unmanned aerial vehicles. Three approaches are presented: Boids Flocking, Potential Fields and Virtual Spring.

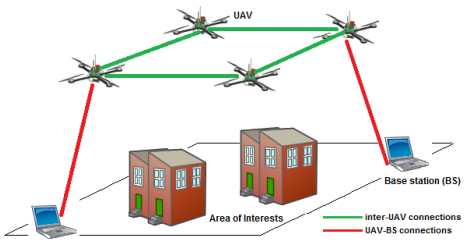

Fig. 1. UAV Ad-hoc Networks Scenario.

The remainder of the paper is organized as follows. In section 2, we describe the latest developments and essential problems of UAV ad-hoc networks. Different application scenarios will be introduced within the section. In section 3, we focus on the topology control of the UAVs ad-hoc networks and three different approaches are described, which can be regarded as the possible solutions for decentralized UAVs topology control. Based on these concepts, our proposed approach is also discussed in this section. Finally, section 4 concludes the paper.

2 UAV Ad-hoc Networks

A mobile ad-hoc network (MANET) is a wireless network that is formed by a collection of self-organizing mobile nodes. Each node communicates with its neighbors over a shared wireless medium. Due to the lack of central management, nodes in MANETs are designed to act as end systems and routers for other nodes. The network is established dynamically and does not rely on any pre-existing network infrastructure. In MANETs, nodes are free to move and have the capability of deliver messages in a decentralized manner. UAVs have the potential of creating an ad-hoc network in the air, namely UAV ad-hoc networks. Most UAVs used in communication networks are equipped with wireless transceivers using omni-directional antennas. In UAV ad-hoc network communication environments, due to the fast mobility of UAVs, network topology may change rapidly and unpredictably. As a result, UAVs are expected to act cooperatively to establish network connections for data routing. When UAVs perform a cooperative task by flying as a group, they can be considered flying in a formation. Formations must safely reconfigure in response to changing missions, UAV density and environment. Additionally, wireless links within a UAV ad-hoc network may alter in link quality over time due to a number of reasons, such as Doppler effects, changes in communication distance, etc. All these requirements make topology control more important in a UAV ad-hoc network environment.

Despite numerous design challenges, there are many application scenarios for UAV ad-hoc networks. Such UAV swarms have a wide variety of applications in both civil and military domains since they are rapidly deployable and highly survivable. There are many separate capabilities for use in addressing application-specific problems: (i) ground sensing; (ii) the ability to bridge communication, etc. Brief examples of these include: search and rescue; chemical/biological/radiological pollution monitoring; disaster recovery, e.g., flooding damage assessment; overflight of sensor fields for the purpose of data collection; and agriculture application[1]. A practical work about the autonomous deployment of a UAV ad-hoc network could be found in [2].

3 Topology Control of UAV Swarms

The absence of central infrastructure implies that an ad hoc network does not have an associated fixed topology. Indeed, an important task of an ad hoc network consisting of geographically dispersed nodes is to determine an appropriate topology over which high-level routing protocols are implemented. Topology control algorithms for wireless ad-hoc networks are mainly based on controlling and adapting the transmission power of nodes. Exploiting the high mobility of nodes, such as UAVs, will bring challenges.

In the following, we will first outline the relationship between coverage and connectivity in UAV ad-hoc networks. After that three mechanisms which might be applied for helping topology control in UAV ad-hoc networks are described.

3.1 Connectivity *versus* Coverage

The novelty of UAV ad-hoc network systems is that the movement of UAVs is controlled by fully autonomous algorithms with two objectives: first to maintain network connectivity to enable real-time communication between UAVs and ground devices; second, to increase sensing coverage to rapidly identify targets. The major resource constraints of using UAVs are battery power, communication bandwidth and processing capabilities. The life time of UAVs and the on-board radio transmission distance are limited. Thus, the behavior of UAV swarms regarding flight routes and communication has to be efficient. Therefore the global requirement of achieving spatial coverage and the local requirement of keeping connectivity could be regarded as contrary to each other. On one hand, high coverage in space is needed for gaining pertinent information from disjunct perspectives that cover a large region of interest. On the other hand, a disruption-free connectivity is indispensable, which mainly depends on the signal degradation due to propagation loss. Hence, the distances in the UAV ad-hoc network configuration must not exceed the receiver's sensitivity and need to be restricted to the boundaries of minimum signal-to-noise-ratio (SNR) or receive signal strength indicators (RSSI) respectively.

3.2 Boids Flocking

Boids flocking [3] is the first and major study on agent-based behaviors. It was the pioneering study where bio-inspired cooperative movements of agents have been developed. Due to its decentralized control mechanism, boids flocking could be considered as a basis to deploy aerial swarms in simulation.

[3] developed a computer animation model for coordinated motion of groups of animals such as bird flocks and fish schools. This flocking model consists of three steering rules that describe how an individual agent(so called "boid") independently maneuvers based on the positions and velocities of its nearby flock-mates (as shown in Figure 2):

- **Separation**: steer to avoid crowding local flock-mates.
- **Alignment**: steer towards the average heading of local flock-mates.
- **Cohesion**: steer to move towards the average position of local flock-mates.

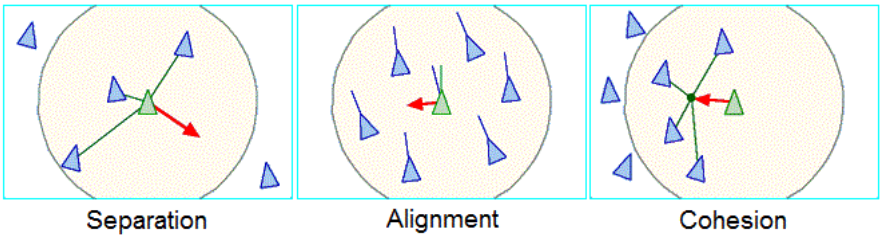

Fig. 2. Local separation, alignment and cohesion on the motion of flocking agents.

Separation could be regarded as collision avoidance, to enable agents be repulsed from neighboring agents to avoid collisions. Alignment enables agents to align their velocities(both speed and direction) to the average of neighboring agents. Cohesion empowers agents to be attracted to the average centroid of neighboring agents to stay close to neighbors. The superposition of these three rules results in all flying agents moving in a formation, with a common heading while avoiding collisions. An extension work of boids flocking is [6], which invented a discrete force model for pedestrian motion.

3.3 Potential Field

Potential field techniques for robotic applications were first described by Khatib in [4] and have been widely used in the mobile robotic community for tasks such as goal seeking and obstacle avoidance.

In this context, objects like goal area or obstacles will be occupied by artificial or virtual potential fields. There are mainly two different types of fields: an attractive potential field, and a rejective potential field. Attractive field corresponds to a seek-goal behavior, and rejective field corresponds to a collision/obstacle avoidance behavior. In general, the repelling forces decrease with distance and the attracting forces increase with distance. The calculation of the type and strength of the potential field created by obstacles, other UAVs or communication infrastructure is based on the agent's sensors. Usually, it can be assumed that the strength of the potential field is inversely proportional to the distance between two objects, as shown in Figure 3*.

3.4 Virtual Spring

A virtual spring-based model is proposed by [5]. According to the model, within a specified neighborhood radius, each vehicle forms a virtual connection with

* http://students.cs.byu.edu/ cs470ta/goodrich/fall2004/lectures/Pfields.pdf.

each neighbor vehicle by a virtual spring. As the vehicle changes its position, speed and altitude, the total resulting forces on each virtual spring try to equal zero by moving to the mechanical equilibrium point. The agents then add the simple total virtual spring constraints to their movements to determine their next positions individually. Together, the multi-agent vehicles reach a group behavior, where each of them keeps a minimal safe-distance with others. A new safe behavior thus arises in the group level. When the spring forces are applied to an agent, the total applied force is defined⋆ as:

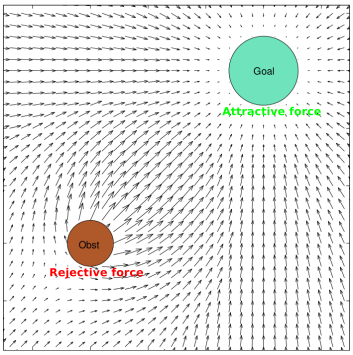

Fig. 3. Potential fields of attractive, rejective and combined.

$$F_{x|y|z} = \sum_{i=1}^{n} \frac{\Delta L_i \times K_i \times (X_i|Y_i|Z_i - X_A|Y_A|Z_A)}{D_i}$$

in which X_A, Y_A, Z_A specify the present position of an agent, n is the number of factors the agent has spring connections with (for this case it is equal to the number of neighbors), L_i is the length of the spring with i^{th} factor, K_i is the constant of that spring, D_i is the distance to the i^{th} factor and (X_i, Y_i, Z_i) specify the position of the i^{th} point.

According to [5], vehicles need no direct communication with each other, require only minimum local processing resources, and the control is completely distributed. However, this is under the assumption that each vehicle knows the neighbors' position, which come from the messages exchange with neighbors.

As a summary, a comparison of three models could be found in Table 1, which lists the pros or cons, and the possible applications of different approaches.

Mechanism	Pros or Cons	Applications
Boids Flocking	*Cons:* Mostly for computer animation.	Connectivity
Virtual Spring	*Cons:* Only distance is utilized, not accurate.	Coverage
Potential Field	*Pros:* Both distance and RSSI are used.	Coverage & Connectivity

Table 1. Comparison of three approaches

3.5 Adaptation of Swarm Control Concepts for Topology Control in UAV Ad-hoc Networks

Since the possibility of connectivity losses can not be absolutely avoided in a UAV ad-hoc network environment, it is essential to ensure the viability of all UAVs and the fulfillment of the overall mission objectives. Subsequently, UAVs within the swarm are designed as autonomous agents, which are capable to react cognitively on environmental changes such as connectivity and sensor perception. On this basis, UAVs should adapt their motion to positions with channel characteristics to provide better network connectivity or coverage.

Based on the concepts described before, we propose to develop a topology control protocol inspired by the potential field approach, with some adaptation.

⋆ $X|Y|Z$ means X or Y or Z.

The strength of the artificial field, which interconnects the UAVs, is calculated dependent on both the RSSI value and distance measured between two UAVs. Our assumption is that, due to the fact that each UAV is equipped with a GPS module, it can broadcast its position to inform the neighbors about their distance. A lower/upper distance bounds between UAVs will be defined. Within these bounds, RSSI signal is utilized to adapt the movements of UAVs. If the RSSI is too low, the force for attracting two UAVs becomes higher, two UAVs will fly close to each other to keep the connectivity. If the RSSI is too high, UAVs are too close and therefore they need to be pushed away from each other. In case of temporary invalid recognition of RSSI, as an alternative, GPS information might still be available and utilized for controlling the movement of UAVs. Besides, to avoid obstacle collisions, in which UAVs can not retrieve any RSSI value from the obstacle, GPS information of the obstacle (i.e., derived from a leading UAV with cameras) will enable UAVs to calculate the distance to steer their movements. Another important design issue is that, in general the inter-reactions between agents of a swarm can only change the relative position of each other within the swarm, and can not modify the movement of the swarm itself. Without any external intervention, the motion of the swarm will keep its initial state, which is unknown in most cases. Therefore, in order to have the swarm moving in an expected manner, it is necessary to control the swarm in a way, i.e., to define a "leader-follower" structure and give commands to the "leader". Interferences and impacts of cross flows will also be considered in the future.

4 Conclusions

In this work, we summarize the mechanisms that could be applied for controlling the movements of mobile ad-hoc UAV swarms. An adaptation of the potential field approach is also presented, which takes into account both distance and RSSI for UAV steering. As a conclusion, topology control in UAV ad-hoc networks must consider application requirements in terms of node density, e.g., when a certain sensing coverage is needed. Alternatively, transmission power can be changed depending on the application in terms of node density and area coverage.

References

1. Costa, F.G., Braun, T., Ueyama, J., Pessin, G. and Santos, F.: Architecture-based Unmanned Aerial Vehicles and Networks of Wireless Sensors for Agricultural Applications. SBIAGRO 2011, Bento Goncalves, Brazil, October 17 - 21, 2011
2. Staub, T.: "Development, Testing, Deployment and Operation of Wireless Mesh Networks", PhD thesis, Chapter 7, pp 153, University of Bern, May 2011
3. Reynolds, C.W.: Flocking, Herds, and Schools: A Distributed Behavioral Model. Computer Graphics, 21(4), ACM SIGGRAPH 1987 Conference Proceedings, pp 25-34, Anaheim, USA, July 1987
4. Khatib, O.: Real-time Obstacle Avoidance for Manipulators and Mobile Robots, International Journal of Robotics Research, 5(1): 90-98, 1986
5. Daneshvar, R. and Shih, L.: Virtual Spring-Based 3D Multi-Agent Group Coordination, in International Conference on Complex Systems (ICCS 2007), Boston, MA, USA, October 28-November 2, 2007
6. Helbing, D., Molnar, P., Farkas, I. and Bolay, K.: Self-organizing pedestrian movement, Environment and Planning B, 28, 361-383, 2001

Performance Assessment of Multi-Operator CoMP in Infrastructure-Shared LTE Networks

Remco Litjens[1], Haibin Zhang[1], Ljupco Jorguseski[1], Bedilu Adela[2], Erik Fledderus[2]

[1] Expertise Centre Technical Sciences, TNO Delft, The Netherlands
{remco.litjens,haibin.zhang,ljupco.jorguseski}@tno.nl
[2] Eindhoven University of Technology, Eindhoven, The Netherlands
{b.b.adela@student.,e.r.fledderus@}tue.nl

Abstract. Cellular networks face important challenges in improving cell edge performance and reducing the costs for network deployment and operation. In recent years improving cell edge performance via so-called Cooperative Multi-Point (CoMP) transmission and reception is receiving significant attention. Another key trend is the reduction of network costs via infrastructure sharing. We investigate the performance benefits of CoMP transmission combined with multi-operator infrastructure sharing, labelled as multi-operator CoMP. These benefits are evaluated for different deployment aspects regarding the degree of co-location of the base stations from different operators and the overlap in their antenna patterns, as well as for different parameterizations of the multi-operator CoMP mechanism. The obtained results indicate that multi-operator CoMP is seen as a promising cell edge performance enhancement feature.

Keywords: Mobile networks, infrastructure sharing, LTE, CoMP, Coordinated Multi-Point.

1 Introduction

Long since the first introduction of wireless networks, interference caused by simultaneous use of the same radio resources has been a major cause for degradation of radio link quality. Several approaches were introduced to create a sufficient amount of isolation between interfering terminals, either in the time, space or frequency domain, or by pre-coding the transmitted signals. It was only in CDMA-based systems that a first form of cooperation was introduced between interfering base stations, using soft handover. Cooperation, or shared resource scheduling among neighbor base stations/cells, has recently received a boost. For example, improving cell edge performance via so-called Cooperative Multi-Point (CoMP) transmission and reception is receiving significant attention [1]-[5]. CoMP is also identified by 3GPP as a technique to improve average and especially cell-edge user throughput for the future releases of LTE [6].

Economical and business incentives have triggered mobile network operators to exploit far-reaching cooperative scenarios. Resource (spectrum and/or infrastructure)

sharing in cellular networks is one of operators' effort to reach this purpose (see e.g. [7][8]), aiming to improve, besides spectral efficiency, the network coverage, to increase user satisfaction, increase revenue for operators, and decrease capital and operating expenditures (CAPEX and OPEX) [9]. Hence, resource sharing may have serious impact on the competition, technical differentiation and future of the mobile market itself. Recent developments show the infrastructure sharing trend in operational cellular networks [10]. According to the GSMA association [11], different levels of infrastructure sharing may be applied, varying from passively sharing the same installation sites, to actively full RAN sharing. Here we address infrastructure sharing where the base stations (including installation sites and base station equipment) of one operator are used by the users of another operator. This is a sort of full RAN sharing, but without sharing spectrum among operators.

Although quite a few publications have addressed CoMP [1]-[6] and resource sharing [7]-[11], respectively, to the authors' best knowledge no assessment has been published of the combined potential of these two techniques. More specifically, all CoMP publications concentrate on a single LTE network scenario. In our view, infrastructure sharing among operators does offer a chance to extend the concept of CoMP to the multi-operator case, in which case sites/sectors of different operators are involved in the CoMP configuration.

Following this novel idea, this paper investigates the performance benefits of configuring CoMP transmission among base stations of multiple operators, in the context of infrastructure sharing. The results published in this paper can serve as a basis for further investigating the pros and cons of this technical approach. The remainder of the paper is organized as follows. Section 2 outlines the research scenario, followed by a description of the system model in Section 3. Section 4 then presents the proposed physical resource sharing and resource assignment algorithms. A quantitative assessment of our proposed solution is given in Section 5. Section 6 concludes with an outlook for remaining challenges.

2 Scenario Description

The basic idea of CoMP is that, by coordinating the transmission and reception of neighboring cells, inter-cell interference is mitigated and the performance of especially cell-edge users is improved. There are different types of CoMP, depending on the means of coordination [1][6]. In this study, we concentrate on downlink CoMP and focus on the so-called 'non-coherent joint transmission CoMP' [2][6]. In this mode, the same data transport blocks are transmitted by multiple cells in the same PRBs (Physical Resource Blocks) to a given terminal. From the terminal's perspective, the signals from different cells are only different in their respective times of arrival, which is to some extent equivalent to the case where the signals are transmitted by a single cell and experience multipath fading.

Traditionally, e.g. in the 3GPP definition so far, CoMP is only configured within one operator's network. However, in the context of infrastructure sharing, it may be advantageous to extend the concept of CoMP to the multi-operator case, in which

case sites/sectors of different operators are involved in the CoMP configuration. As exemplified in Figure 1, in some cases a base station of Operator B may be able to contribute better to enhancing a given terminal's connection, than an additional base station of Operator A, in the sense that it may provide a stronger radio link to the terminal. Such inter-operator cooperation requires that the same data can be transmitted using the same PRBs that are assigned to the terminal by the serving home operator base station. To support this, the base stations/sectors of Operator B must be able to utilize the spectrum of Operator A. In the presented study, we assume that the spectrum of Operator A is only used to serve customers of Operator A, potentially in cooperation with one or more base stations of Operator B. Such inter-operator CoMP configuration can be seen as a way of infrastructure (but not spectrum) sharing, since terminals of one operator make use of the infrastructure (base stations) of another operator while solely using their home operator's spectrum.

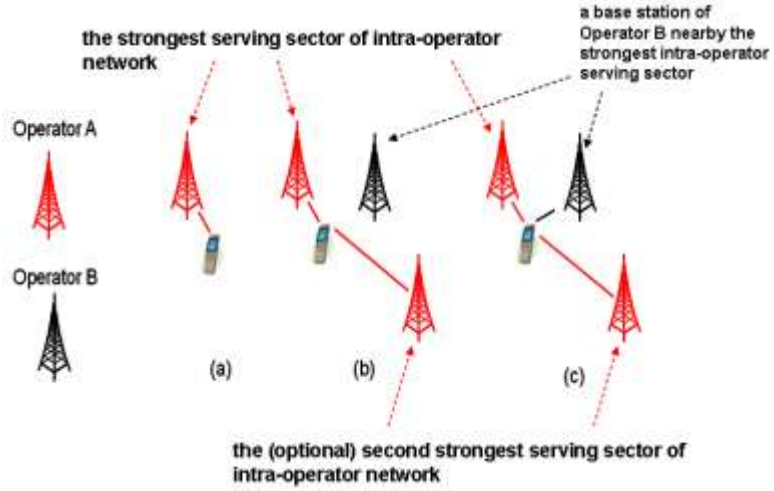

Fig. 1. Illustration of different transmission and reception schemes: (a) single cell transmission; (b) intra-operator CoMP; (c) inter-operator CoMP.

3 System Model

In this section we describe the key modeling aspects regarding network layout, propagation environment and traffic characteristics. Key simulation parameters are given in Table 1.

We consider two network operators each running an LTE-Advanced network comprising twelve sectorized (12×3) sites that are organized in a hexagonal layout, as depicted in Figure 2. A wraparound technique is applied to mimic infinite networks and avoid boundary effects. The degrees of co-siting and 'co-azimuthing' are denoted Δ_{CS} and Δ_{CA}, respectively, and are defined in the figure. Note $\Delta_{CS} = \Delta_{CA} = 0$ corresponds with a scenario of fully co-sited and -azimuthed networks. The antenna dia-

gram is taken from [12]. The propagation environment is characterized by distance-based path loss, shadowing and indoor penetration loss. The key propagation parameters are summarized in Table 1. The considered LTE-A networks serve data flows only, which are modeled as the download of file with a lognormally distributed size with mean 1.0 Mb and a standard deviation of 1.5 Mb. Flows that associated with customers of network operator A are generated according to a spatially uniform Poisson process with average arrival rate λ. Upon generation of a new flow, the main serving cell is determined as the cell in the home network (A) towards which the flow has the highest path gain. Subsequently, the flow's active set is constructed (as outlined in Section 4.2). On-going flows are assigned resources according to the scheme outlined in Section 4.3, which also describes how each flow's signal-to-interference-plus-noise ratio (SINR) is calculated and the effective throughputs are derived. Once all bits of a flow are transferred and hence a download is completed, the flow disappears from the system and its experienced throughput is processed for performance statistics. It is noted that no flow arrival process is modeled for network B, since in the considered scenario of pure infrastructure sharing this does not affect the performance experienced by flow in network A. As will be explained below, the infrastructure of network B is utilized to better serve network A's flows by means of multi-operator CoMP, using network A's frequency spectrum.

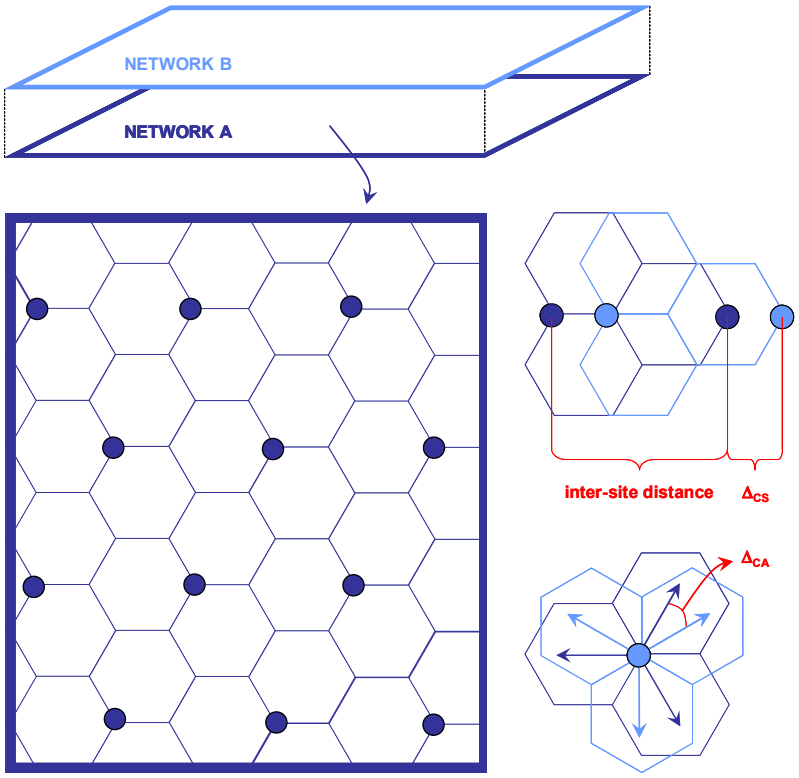

Fig. 2. Network layout.

Table 1. Key simulation parameters.

Inter-site distance	1.0	km
Main lobe antenna gain after cable/slant loss	11.5	dBi
Maximum transmit power[1]	46.0	dBm
Noise power density (per PRB)	-121.5	dBm
Noise figure	8.0	dB
Carrier frequency	2100	MHz
Path loss	$138.5 + 32.23 \log_{10}(d_{km})$	dB
Shadowing standard deviation	8.0	dB
Intra-site shadowing correlation	1.0	
Inter-site shadowing correlation	0.5	
Penetration loss	17.0	dB
Average flow size	1.0	Mb
Standard deviation of flow size	1.5	Mb

4 Resource Management

In this section a number of relevant resource management mechanisms are described, including the formation of cell clusters for CoMP application, the construction of active sets and the allocation of radio resources and user bit rates.

4.1 Intra-/inter-operator CoMP cluster formation

The application of CoMP requires that disjoint clusters are formed comprising multiple cells that may cooperate to jointly serve selected users. Such clustering is needed to allow localized (at the cluster level) and conflict-free resource allocation. Associated impact on control overhead and backhaul requirements, impose a limitation as to the number of cells that can be grouped in such a cluster [2]. In our approach we make use of static intra- and inter-operator cell clusters which are formed as follows. Intra-operator clusters comprise three sectors that either belong to neighboring sites (‘different-site intra-operator cluster’) or to the same site (‘same-site intra-operator cluster’), as illustrated in Figure 3.

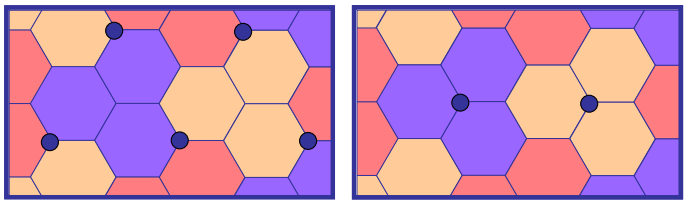

Fig. 3. Different-site (left) versus same-site (right) intra-operator clustering.

[1] The maximum transmit power is assumed available to a cell both for serving its own flows, and for serving the other operator’s flows in inter-operator CoMP mode.

Similarly there is a need for the formation of inter-operator clusters, in order to avoid resource allocation conflicts when resource allocations determined at the intra-operator cluster level, are 'copied' to any supporting cells in the other network (see below). The construction of inter-operator cluster is somewhat more challenging since the clustered sectors belong to two distinct networks with potentially very different network layouts in terms of site locations and antenna orientations. To overcome this challenge we developed a specific inter-operator clustering algorithm, which aims at forming clusters that provide the largest performance enhancement potential and essentially works as follows. Consider the construction of inter-operator clusters from the perspective of network A, which determines for each intra-operator cluster in network A an associated set of cells in network B that are candidates for co-serving flows in network A in a multi-operator CoMP fashion. The construction of inter-operator clusters from network B's perspective is done equivalently. Although this approach may not guarantee a one-to-one correspondence between the inter-operator clusters generated from both perspectives, this is irrelevant, considering the distinct spectrum that is used in each network and those cells invited to co-serve its flows in a multi-operator CoMP fashion.

In order to form these clusters, a large number of user positions are sampled. For each such a position, the best serving cell in both networks A and B are determined. Such a sample indicates an 'association' between the intra-operator cluster containing the best serving cell in network A, and the best serving cell in network B. This association holds in the sense that a terminal at the sampled location is likely to benefit from a configuration where the selected best serving cells in both networks would be able to cooperate in a CoMP fashion. Such an identified association is then a trigger to configure the inter-operator clusters to support such cooperation. After evaluating and processing all sampled user positions, the degree of association between each intra-operator cluster in network A and each individual cell in network B is expressed by the number of observed 'associations'. From the perspective of a given intra-operator cluster in network A, the associated inter-operator cluster in network B then comprises all cells (in network B) whose degree of association is strongest with the given intra-network cluster.

4.2 Active set construction

Given a flow's uniformly sampled location and the corresponding path gains it experiences towards all sectors, the flow's active set (AS), defined as the set of concurrently serving sectors in both its home (A) and host network (B) is constructed as follows. First, the strongest serving cell in the home network A is selected based in the observed RSRPs (Reference Signal Received Power). In scenarios with an activated CoMP feature, subsequently, the active set may be expanded by adding other candidate cells that belong to the intra- or inter-operator cluster corresponding with the selected strongest serving cell. More specifically, the strongest $AS_{max} - 1$ cells are included in the active set, provided that the measured RSRP is at most $\Delta_{AS,intra}$ or $\Delta_{AS,inter}$ worse than that of the strongest serving cell, considering candidate cells of the home and host network, respectively. By setting $\Delta_{AS,inter}$ lower than $\Delta_{AS,intra}$ some

preference is effectuated towards including home over host network cells in a flow's active set. Cells of the host network are then only involved if the achieved performance enhancement is expected to be sufficiently large. Note that setting $\Delta_{AS,intra} = 0$ dB ($\Delta_{AS,inter} = 0$ dB) does not necessarily switch off intra-operator (inter-operator) CoMP entirely, considering the equal link qualities that a given user may have towards co-sited/azimuthed (intra/inter-operator) sectors. Note that settings of the active set construction parameters influence the fraction of users that is served in (intra/inter-operator) CoMP mode.

4.3 Packet scheduling and rate assignments

The proposed resource fairness-oriented packet scheduling scheme is in charge of assigning PRBs to active flows, and operates at flow arrival and departure instants. As the CoMP feature allows given flows to be simultaneously served by multiple cells, coordinated packet scheduling is needed across the intra-network cluster to ensure that a given UE is assigned the same set of PRBs in all its serving cells. The proposed scheduling scheme applies an iterative procedure as outlined in the flowchart of Figure 4, and described below. In an actual network deployment, it would likely be implemented following a master-slave concept. In such an implementation each intra-network cluster features a master site which is maintaining active set information for all flows served by the cluster, perform packet scheduling (see below) and inform the other involved sites (slaves) of the derived PRB assignments. As scheduling decisions are triggered only by flow arrival/departure events, the amount of signaling load on the cluster backbone is quite modest, and any involved signaling delays are tolerable.

To limit the complexity of explanation, the given description of the scheduling algorithm assumes that all flows have sufficient data in the eNodeB buffer to utilize all assigned PRBs. Straightforward adjustments of the algorithm apply in case near-empty buffers make this assumption invalid. Initialize for each cell i in the (intra-network) cluster the number of unassigned PRBs to $n_{PRBs,i} = 50$ (assuming a spectrum availability of 10 MHz). For each flow that is served by one or more cells in the cluster, mark which are its serving cells, which initializes for each cell i the number of unscheduled flows nflows,i. The iteration step is then to select the most resource-limited cell, i.e. the one with the smallest ratio of $n_{PRBs,i} / n_{flows,i}$. For this cell the scheme then assigns $n_{PRBs,i} / n_{flows,i}$ PRBs to each served flow. For flows in CoMP mode (active set size > 1) this PRB assignment is copied to any other serving cells in the cluster. Subsequently, the served flows are marked as 'scheduled', the values of $n_{PRBs,i}$ and $n_{flows,i}$ are updated accordingly in each cell and the iteration step is repeated until all flows are scheduled. Note that due to the CoMP restrictions, this does not necessarily imply that all PRBs are assigned.

As an illustration of the scheme, consider the scenario with five flows served by a three-cell cluster in network A given in Table 2. See also Figure 5. Note that flows 2 and 5 are in CoMP mode. According to the scheduling scheme, in the first iteration, CELL A_I has the smallest $n_{PRBs,i} / n_{flows,i}$ ratio ($50 / 3 < 50 / 2 = 50 / 2$) and hence 50 / 3 PRBs are assigned to its three served flows. In the second iteration, CELL A_{II} is addressed ($50 / 2 < (50 – 50 / 3) / 1$) and hence 50 / 2 PRBs are assigned to flows 4

and 5. Since all flows are scheduled, the scheme terminates. Note that in CELL A_{III} some PRBs remain unassigned, a drawback which is due to the CoMP-imposed restrictions.

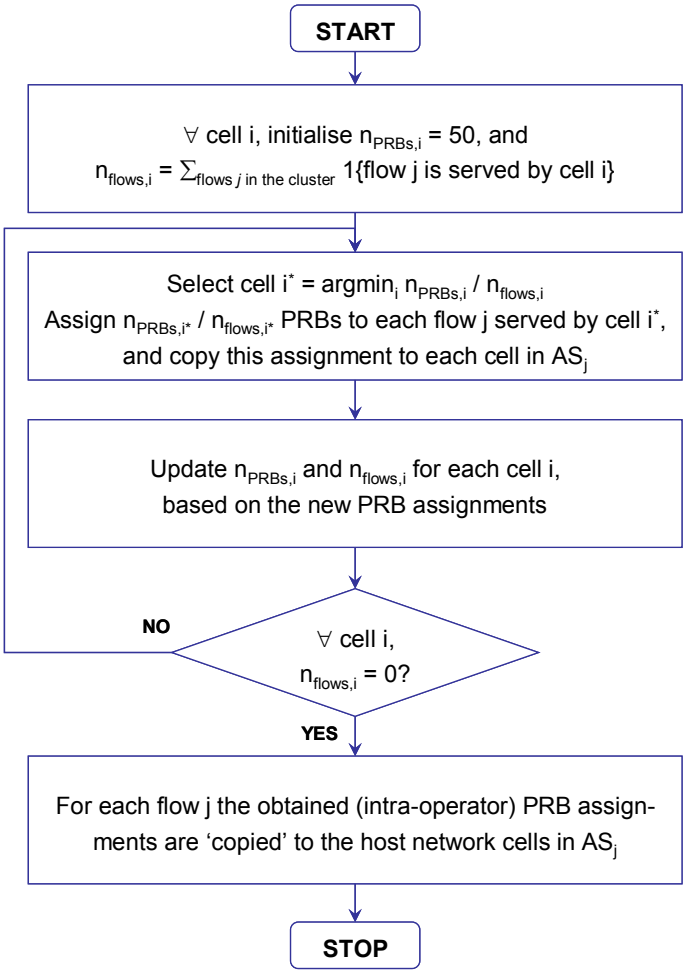

Fig. 4. Flowchart of the proposed CoMP-based packet scheduling scheme for infrastructure-sharing networks.

Table 2. Packet scheduling example.

	CELL A_I	CELL A_{II}	CELL A_{III}
FLOW 1	V		
FLOW 2	V		V
FLOW 3	V		
FLOW 4		V	
FLOW 5		V	V

The obtained (intra-operator) PRB assignments are 'copied' to the involved cells in the host network. Suppose in the example that the active set of FLOW 4 comprises, besides CELL A_{II}, also CELL B_{III} in network B. Then FLOW 4 is simultaneously served by both cells on the same 25 PRBs that have been assigned in the above procedure. Given the construction of inter-operator cell clusters, this does not lead to any conflicts. *Note further that the frequency band in which network B supports network A via multi-operator CoMP is different from that in which network B serves its own flows (potentially supported by network A) and hence supporting another network in inter-operator CoMP mode imposes no resource limitations and performance effects towards a network's 'own traffic'.*

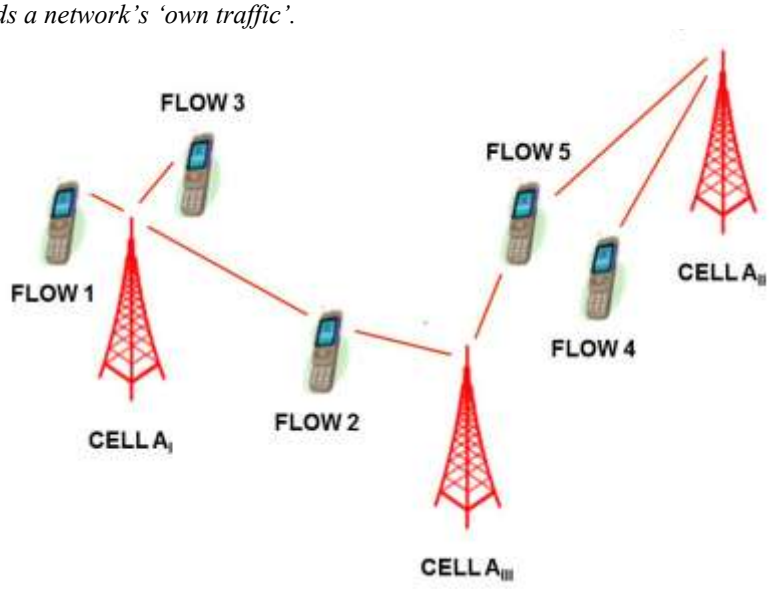

Fig. 5. Packet scheduling example.

Given the PRB assignments determined by the packet scheduler, the flow-specific bit rates are derived as follows. Firstly, the radio link quality of active flow i served by active set AS_i is given by its experienced SINR (signal-to-interference-plus-noise ratio), which for PRB j is calculated as follows:

$$SINR_{ij} = \frac{\sum_{b \in AS_i} P_{bj} G_{bi}}{\sum_{b' \notin AS_i} P_{b'j} G_{b'i} + N},$$

where P_{bj} denotes sector b's current transmit power in PRB j and G_{bi} denotes the total path gain between sector b and user (flow) i. The correspondingly attainable bit rate (in Mb/s) is then given by [11]

$$R_{ij} = 0.18 \cdot \min\left\{4.4, 0.6 \cdot \log_2\left(1 + SINR_{ij}\right)\right\},$$

while the flow's total rate is summed over the assigned PRBs.

5 Numerical Results

In this section, simulation results are presented based on the system model and resource management mechanisms described in Section 3 and Section 4, respectively. Two key performance indicators are used: average flow throughput and cell edge average flow throughput. The cell edge is defined by a path loss threshold, chosen such that 10% of the flows are considered cell edge flows. A flow for which the sum of distance-based path loss, shadowing, indoor penetration loss and antenna gain towards its strongest serving cell exceeds the path loss threshold is labeled as a cell edge flow.

5.1 Performance gains from inter-operator CoMP

In this subsection we analyze the gains of inter-operator CoMP with regard to both single-cell transmission and intra-operator CoMP. The following parameter configurations are assumed: $AS_{max} = 3$, $\Delta_{AS,intra} = \Delta_{AS,inter} = 3$ dB and $\Delta_{CS} = 0$ (co-sited). Since $\Delta_{AS,inter} = \Delta_{AS,intra}$, cells of the host network have the same priority as those of the home network in being involved in any flow's active set. Two degrees of co-azimuthing are considered for the two networks, viz. $\Delta_{CA} = 0^o$ (co-azimuthed) and $\Delta_{CA} = 60^o$ ('anti-azimuthed'). The comparison between different degrees of co-azimuthing is of particular interest, considering that in current practices of co-siting among operators, sectors of different operators may typically have different azimuths. Both different-site and same-site intra-operator clustering configurations are considered.

Figure 6 shows the comparison between single-cell transmission, intra-operator CoMP and inter-operator CoMP in average flow throughput (left chart) and cell edge average flow throughput (right chart), at different cell loads and for the different-site intra-operator clustering configuration. The following observations can be made from the figures:

- Intra-operator CoMP has little or even no gain in average flow throughput over single-cell transmission, while the cell edge average flow throughput is significantly improved. This is in line with the design objective that intra-operator CoMP mainly benefits cell edge flows, for which the probability of having more than two cells in their active sets is higher than that of cell center flows.
- Inter-operator CoMP with co-azimuthed configuration has significant gain in both average flow throughput and cell edge average flow throughput over both single-cell transmission and intra-operator CoMP. For example, at the cell load of 11 Mb/s, it has 22% (21%) higher average flow throughput and 39% (24%) higher cell edge average flow throughput over single-cell transmission (intra-operator CoMP). This is largely due to the fact that, with co-sited and co-azimuthed configuration, the host network cell which is co-sited and co-azimuthed with the strongest home

network serving cell of each flow (no matter where in the cell) will have the same measured RSRP as the strongest home network serving cell, and thus will be included in the active set of the flow and significantly improve the performance. So all the flows are in inter-operator CoMP mode.

- Inter-operator CoMP with 'anti-azimuthed' configuration has even lower average flow throughput than those of single-cell transmission and intra-operator CoMP. For cell edge average flow throughput, it outperforms single-cell transmission and slightly over intra-operator CoMP. It is outperformed by inter-operator CoMP with co-sited and co-azimuthed configuration on both performance metrics. This is largely due to the fact that, with co-sited and 'anti-azimuthed' configuration, and applying different-site intra-operator clustering, for some flows the host network cell for which the measured RSRP is the strongest might not be in the same cluster where the flow is served. Consider for instance a user located 'in between' a home network site's cells A and B. Assume he is served by cell A and hence, considering the applied intra-operator clustering, not also by cell B. Co-sited host network cell C with an azimuth 'in between' cells A and B is likely to be in the same cluster with either cell A or B. In case of the latter, the given user cannot include it in its active set yet may experience a rather significant degree of interference from cell C, which may support cell B in a multi-operator CoMP fashion. The impact of this source of interference is likely to be larger for cell center than for cell edge flows.

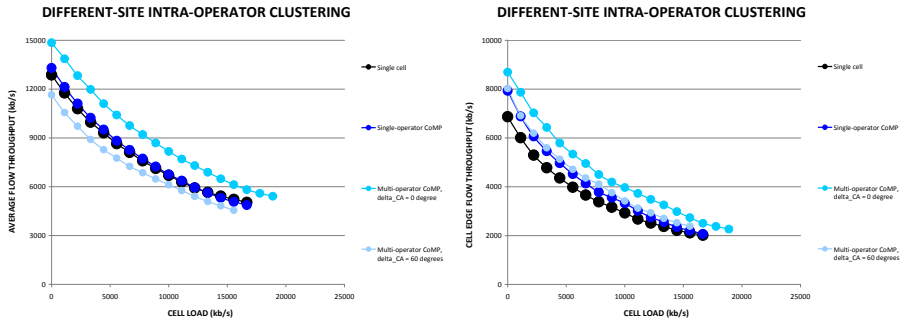

Fig. 6. Average (left) and cell edge average flow throughput vs traffic load: single-cell transmission, intra- and inter-operator CoMP (different-site intra-operator clustering).

Since CoMP mainly aims at improving the performance at cell edge, in the following discussions we will focus more on the impact of intra-/inter-operator CoMP, with different configurations, to the cell edge average flow throughput. Figure 7 (left chart) shows a performance comparison of the single-cell transmission and intra/inter-operator CoMP modes for the same-site intra-operator clustering configuration. The following observations can be made:

- Intra-operator CoMP offers only a little gain in cell edge average flow throughput over single-cell transmission, much lower than that for the different-site intra-operator clustering configuration. The reason is that, for most cell edge flows, the neighbor cells which may help best in improving their performance are not in the

same cluster and hence no CoMP candidates. Instead of serving the cell edge flows, they may in fact be strong interferers if they serve flows in other clusters using the same spectrum.

- Inter-operator CoMP outperforms both single-cell transmission and intra-operator CoMP, for both degrees of co-azimuthing. For example, at a cell load of 11 Mb/s, inter-operator CoMP yields about 33% (39%) higher cell edge average flow throughput compared to the case of intra-operator CoMP, for the co-azimuthed ('anti azimuthed') configuration. The degree of co-azimuthing does not significantly impact the cell edge average flow throughput. For the same-site intra-operator clustering, the change of co-azimuthing degree in fact does not change the inter-operator clustering, and for the majority of flows the active sets are the same. The minor difference in performance is due to the directional antenna pattern, because of which the radio condition for some flows changes slightly with the co-azimuthing degree.

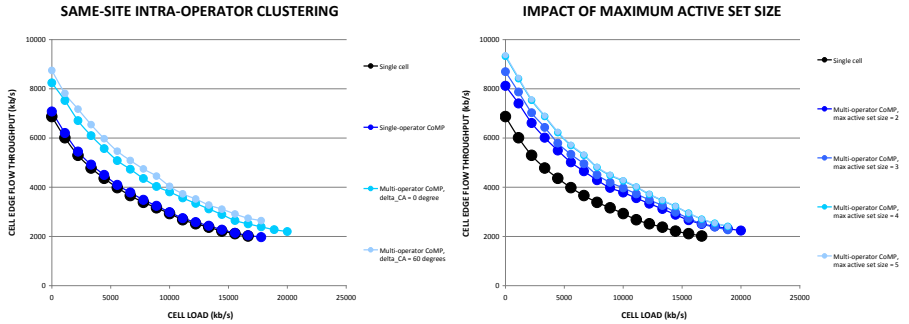

Fig. 7. Cell edge average flow throughput vs traffic load (same-site intra-operator clustering; left chart). Performance impact of AS_{max} (right chart).

5.2 Sensitivity analysis of the CoMP performance gains

We now analyze the sensitivity of the inter-operator CoMP performance with regard to AS_{max}, $\Delta_{AS,inter}$, $\Delta_{AS,intra}$ and Δ_{CS}. The impact of each parameter was investigated in a ceteris paribus setting, assuming a common baseline configuration, given by a different-site intra-operator clustering, $AS_{max} = 3$, $\Delta_{AS,inter} = \Delta_{AS,intra} = 3$ dB and $\Delta_{CA} = 0^o$ (co-azimuthed).

Figure 7 (right chart) shows the impact of AS_{max} on the cell edge average flow throughput. The general trend is that a higher AS_{max} yields a better performance up to an AS_{max} of about 4, beyond which further gains are negligible (the maximum value of AS_{max} is limited by the total cluster size, which is 6 in our case). One reason is that even with higher AS_{max}, the actual active set size of flows might not be higher due to the limitation of $\Delta_{AS,inter}$ and $\Delta_{AS,intra}$. Another reason is that, even the actual active set size of some flows becomes higher with higher AS_{max}, the extra cells involved in the active set contribute little to the overall SINR due to their relatively low link qualities.

Figure 8 (left chart) shows the performance impact of $\Delta_{AS,intra}$. The general trend is that better performance is achieved for higher $\Delta_{AS,intra}$. However, the performance for

$\Delta_{AS,intra}$ = 3 dB is almost identical to that for $\Delta_{AS,intra}$ = 2 dB, which indicates that further increase of $\Delta_{AS,intra}$ will not benefit the performance further. Note that inter-operator CoMP with $\Delta_{AS,intra}$ = 0 dB yields a significant performance gain over single-cell transmission. The reason is that in a co-sited and co-azimuthed network configuration, the host network cell which is co-sited and co-azimuthed with the strongest home network serving cell of each flow (regardless of its precise location) will be included in the active set of the flow (even when $\Delta_{AS,intra}$ = 0 dB) and hence significantly improves the performance.

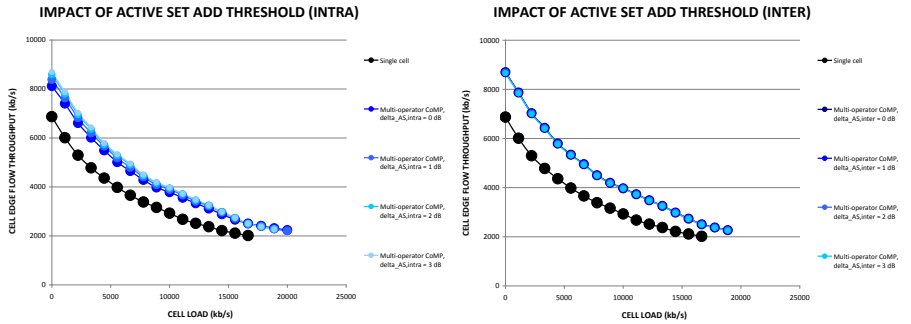

Fig. 8. Performance impact of $\Delta_{AS,intra}$ (left chart) and $\Delta_{AS,inter}$ (right chart).

Figure 8 (right chart) shows the performance impact of $\Delta_{AS,inter}$. The general trend is that worse performance is experienced with a lower $\Delta_{AS,inter}$. However, when $\Delta_{AS,inter}$ is decreased from 3 dB to 0 dB, the performance is only affected marginally. The reason is that, with a co-sited and co-azimuthed configuration, the host network cell which is co-sited and co-azimuthed with the strongest home network serving cell of each flow (regardless of its precise location) will be included in the active set of the flow for this range of $\Delta_{AS,inter}$.

Figure 9 shows the impact of Δ_{CS}, which to some extent influences the performance of inter-operator CoMP. It is noted that Δ_{CS} is expressed in units equal to the inter-site distance. In general, it is hard to predict what Δ_{CS} would be optimal, since for each 'choice' of Δ_{CS} a different set of user locations would benefit most from inter-operator CoMP. The curves indicate that, apparently, the cell edge flow throughputs are most improved, considering moderate to heavy loads, for a Δ_{CS} around 0.083 × the inter-site distance. The most interesting observation is that inter-operator CoMP always outperforms single-cell transmission (and also intra-operator CoMP according to Figure 13), for all the investigated values of Δ_{CS}. Hence even in a situation of non co-siting, infrastructure sharing via inter-operator CoMP is still beneficial.

6 Concluding Remarks

We investigated the benefits from inter-operator CoMP downlink transmissions as an extension to the 'traditional' intra-operator CoMP feature in LTE-Advanced networks. In order to assess the potential performance gains, we have proposed and as-

sessed procedures for defining inter-operator cell clusters, an intra- and inter-operator cell selection mechanism for inclusion in CoMP transmissions and coordinated inter-operator scheduling. The assessment study focused on different deployment scenarios with regards to the site locations (e.g. co-sited versus non co-sited) and antenna orientations (e.g. co-azimuth versus non co-azimuth orientation).

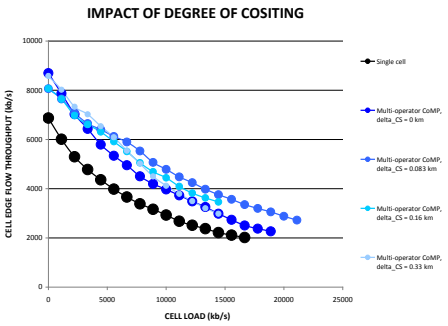

Fig. 9. Performance impact of Δ_{CS}.

The results show that inter-operator CoMP can achieve average flow throughput and cell edge flow throughput gains of 21% and 24%, respectively, over intra-operator CoMP for the case of co-azimuth antenna orientation and under a moderate cell load. The average flow throughput performance for the inter-operator CoMP degrades only in the case of non co-azimuth antenna orientation (it is even worse than intra-operator single cell transmission without CoMP) due to the interference from inter-operator cells that is caused by the exclusion of such cells from the inter-operator cluster which is due to the different antenna orientation. Further, it is shown that the active set size up to four intra- or inter-operator cells is sufficient to extract the most of the inter-operator CoMP gains. The inter-operator CoMP performance is rather insensitive to the active set thresholds for inclusion of intra- or inter-operator cells of up to 3 dB. Finally, inter-operator CoMP is outperforming intra-operator CoMP in terms of average and cell edge flow throughput also for the case of non co-siting.

Due to the observed throughput benefits the inter-operator CoMP can become an interesting mechanism for infrastructure sharing among cooperating operators. It is recommended as a follow-up study to evaluate the added complexity in terms of inter-operator signaling and impact on the backhaul networks imposed by using inter-operator CoMP, in order to further assess the suitability of this feature for practical deployments.

Acknowledgments

This work has been performed in the framework of the European research project SAPHYRE [9], which is partly funded by the European Union under its FP7 ICT Objective 1.1 - The Network of the Future.

References

1. J. Zhu et al, ‘A practical design of downlink coordinated multi-point transmission for LTE-Advanced’, Proceedings of VTC ‘10, Taipei, Taiwan, 2010.
2. S. Brueck et al, ‘Centralized scheduling for joint transmission Coordinated Multi-Point in LTE-Advanced’, Proceedings of WSA ‘10, Bremen, Germany, 2010.
3. P. Marsch et al, ‘Field trial results on different uplink coordinated multi-point (CoMP) concepts in cellular systems’, Proceedings of Globecom’10, Miami, Florida, USA, 2010.
4. Q. Wang et al, ‘Coordinated multiple points transmission for LTE-Advanced systems’, Proceedings of WiCom’09, Beijing, China, 2009.
5. V. Jungnickel et al, ‘Coordinated Multipoint Trials in the Downlink’, Globecom work-shop’09, Honolulu, Hawaii, USA, 2009.
6. 3GPP TR 36.819, ‘Coordinated multi-point operation for LTE physical layer aspects’, v11.0.0, 2011.
7. Www.net4mobility.com, 2011.
8. Telecoms.com, ‘Orange and Play to form Polish joint venture’, www.telecoms.com/22382/ orange-and-play-to-form-polish-jv/, 2011.
9. FP7 SAPHYRE project, ‘Sharing physical resources - Mechanisms and implementations for wireless networks’, www.saphyre.eu, 2011.
10. Infrastructure sharing, ICT regulation toolkit. http://www.ictregulationtoolkit.org/en/Sec-tion.3440.html.
11. Infrastructure sharing, GSMA association. http://gsm.org/our-work/public-policy/ regula-tory-affairs/infrastructure_sharing.htm.
12. 3GPP TR 36.942, ‘Evolved Universal Terrestrial Radio Access (E-UTRA); Radio Fre-quency (RF) system scenarios’, v8.1.0, 2008.

Modeling and Evaluation of LTE in Intelligent Transportation Systems

Konstantinos Trichias[1], Hans van den Berg[1,2], Geert Heijenk[2], Jan de Jongh[3], Remco Litjens[1]

[1]Performance of Networks & Systems (PoNS), TNO, Delft, The Netherlands
{kostas.trichias,j.l.vandenberg,remco.litjens}@tno.nl
[2] Department of Computer Science, University of Twente, The Netherlands
geert.heijenk@utwente.nl
[3]Network Technology (NT), TNO, Delft, The Netherlands
jan.dejongh@tno.nl

Abstract. The term *Intelligent Transportation Systems* (***ITS***) refers to adding information and communications technology to transport infrastructure and vehicles. The IEEE 802.11p standard is considered the main candidate for communication within the context of ITS and it performs well for active safety use cases thanks to its very low delay. Nonetheless, there are still some problems that originate mostly from the decentralized ad-hoc nature of the protocol, that lead us to believe that the information exchange in ITS can also be handled via a different kind of network. In this paper, the technical feasibility of the use of LTE for ITS communication is examined. A model was built simulating the function of the LTE evolved Radio Access Network (eRAN) operating in a vehicular environment and its performance is evaluated. The results are encouraging and indicate that LTE can be used to handle certain types of traffic in a vehicular network.

Keywords: LTE, ITS, 802.11p, vehicular communications

1 Introduction

The IEEE 802.11p standard [1] is considered to be the future of Vehicular Ad-hoc Networks (VANETs) and is capable of providing vehicle-to-vehicle (V2V) and Infrastructure-to-Vehicle (I2V) communications. The standard will be used for communications within the concept of ITS, and will support safety, traffic efficiency and infotainment applications such as collision avoidance, traffic avoidance, commercial applications and others. The 802.11p is suitable for vehicular communications mainly due to its very low end-to-end delay, which is a crucial factor for ITS applications, especially for the ones which aim at road and vehicle safety and hence, have very stringent timing requirements. A comprehensive list of ITS classes, applications and requirements can be found in [2]. Nonetheless, 802.11p also faces some severe prob-

lems which mainly originate from its decentralized ad-hoc nature, and degrade its performance significantly in some cases. Some of the most important problems are: the hidden node problem, the scalability issues, the degradation of performance under high mobility of the nodes and the use of optimal transmit power by the nodes in order to minimize interference.

These issues, make apparent the need for a search for an alternative communications protocol that will either assist or replace 802.11p for use in ITS. The 3rd Generation Partnership Project (3GPP) Long Term Evolution (LTE) is an attractive solution mainly due to its extraordinary performance and the fact that it is an infrastructure-based communications system, thus, not facing the same problems as 802.11p. LTE's extraordinary features such as the extremely low end-to-end delay, the high data rates, the large communication range and the fact that it is readily available (commercial networks are already being operational or deployed), make it an ideal candidate for use in ITS networks.

This paper presents the work carried out in [3], in which the performance boundaries of LTE technology in relation to the requirements of typical ITS applications are explored. Moreover, the way that the different parameters of the vehicular network, such as vehicle density and beaconing frequency, affect the performance of LTE is investigated. Furthermore, the effect that the introduction of LTE in ITS has on existing cellular traffic is examined and different possibilities for improving the performance of LTE in the ITS context are investigated.

The remainder of this paper is organized as follows. In section II the model that was used to evaluate the performance of LTE in ITS networks is described, the simulation scenarios are presented and the simulation choices that were made, are motivated. In section III the radio resource management is discussed. The calculation of the users bit rate and the effect of the mobility of the nodes is explained and the transmit power control, retransmission and scheduling schemes are presented. In section IV the simulation results are presented and analyzed while the performance of LTE is evaluated. Finally, in section V we draw our conclusions based on the simulation results.

2 Model Description

Before going any deeper into the details of the model, we have to motivate some of the basic modeling choices that were made. In general, the LTE downlink (DL) path, meaning the communication from the evolved Node B (eNB) to the user equipment (UE) tends to perform better than the uplink (UL) path (UE→eNB), thus offering higher throughput and smaller delays. This is mainly due to the fact that the DL is heavily dependent on the eNB which offers great transmission and computational power. The eNB can use a more advanced Multiple Input Multiple Output (MIMO) scheme, since it has more transmit antennas and can also make use of broadcasting. On the other hand, the UL is heavily dependent on the UE, meaning restricted transmission and computational power, limited battery life and a simpler MIMO scheme for transmission. For these reasons, we consider the UL to be the bottleneck of the

system, especially when used in the highly dynamic vehicular environment, so we chose to focus on modeling the UL in detail. The DL on the other hand was simulated by a simple broadcast scheme, which is reasonable since that is the way that ITS applications operate (one vehicle transmitting to multiple neighboring vehicles).

The function of a LTE network operating in a vehicular environment was simulated by a model created within TNO using the Borland Delphi programming language. The environment that our model simulates and its basic principles are depicted in Figure 1. The vehicles communicate with each other over a commercial LTE network (ITS traffic), at the same time that other mobile users are establishing data connections with the same network (background traffic). The vehicular environment simulated is a rural highway with multiple lanes and a variety of traffic patterns. The LTE part of the model simulates the function of a LTE cell operating in the 900 MHz band with a bandwidth of 10 MHz. The eNB of the cell is situated in the middle (lengthwise) of the simulated highway, at a height of 30 meters and uses an omni-directional antenna. LTE serves both vehicular and background mobile telephony users at the same time and it has to meet the Quality of Service (QoS) requirements for each service, respectively, although in our scenario no QoS is taken into consideration for the background traffic.

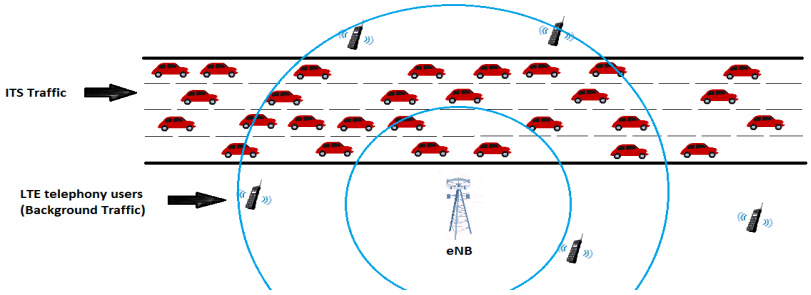

Fig. 1. Basic modeling scenario

In this basic simulation scenario that is presented in Figure 1, all the vehicles participate in an ITS and exchange periodic messages with each other through the eNB. Because these messages have predefined size and are generated at regular intervals, they are called *beacons*, and the frequency with which they are transmitted is called *beaconing frequency*. Each beacon transmitted by each vehicle has to reach the eNB and go through the whole LTE network before it can be delivered to the rest of the ITS users, through a broadcast transmission by the eNB. In our scenario only one cell (eNB) is taken into account, so there is no rebroadcasting from neighboring eNBs.

For the creation of the road network and the simulation of the movement of the vehicles, the Intelligent Driver Model (IDM) developed by Treiber, Hennecke and Helbing was used [4] [5]. In traffic flow modeling, the IDM is a time-continuous car-following model for the simulation of freeway and urban traffic. In our model, the initial positions and velocities of the vehicles were taken from a uniform distribution and they were recalculated with a refresh rate of 100 ms, which ensured that the model adapts well to the changes of the channel. Moreover, the IDM was updated in order

to allow for the creation of multiple lanes (for traffic towards the same direction) and the insertion of traffic jams, in order to simulate realistic traffic patterns.

Every vehicle on the highway transmits a beacon of predefined size with a fixed beaconing frequency. The most common value for the beacon size is 100 Bytes and the most common beaconing frequency is 10 Hz, but the values of these parameters change depending on the ITS application that is served. Here, we will examine only the case of the periodic beacon transmission from the vehicles and not the case of event triggered messages (see[2]).

In our model, each vehicle picks a random initial time to generate its first beacon from a uniform distribution, and after the generation of the first beacon, all the subsequent beacons follow in fixed time intervals depending on the beaconing frequency (a beaconing frequency of 10 Hz leads to a beacon inter-arrival time of 100 ms). Then, the ITS users have to wait for the eNB to assign resources to them depending on the scheduling scheme that is implemented (see Section III), in order to be able to transmit their beacon. The UL transmission delay of the beacon is defined as the elapsed time from the generation of the beacon until the transmission of the last bit of the beacon. For the DL path (eNB→UEs), a broadcast transmission was assumed and the broadcasting bit rate was adapted to the receiver with the weakest signal. So, the vehicle with the lowest bit rate (which is usually the vehicle situated farthest away from the eNB) at any given moment, defines the bit rate of the broadcast transmission and hence the DL transmission delay. The rest of the path that a packet travels through the LTE network was not simulated, but some typical values regarding the delay of the packet were taken into account from [6]. So, a core network delay of 2 ms was used, the processing delay both at the eNB and the UE was set at 4 ms and the buffering delay at the UE was set at 1 ms. The transition delay for the UE between idle and active states, which is usually around 100 ms, was not taken into account since it is assumed that the continuous beacon transmissions will keep the UEs in the connected state. By adding the above mentioned delay components we can calculate the end-to-end delay of each beacon in the system.

The background traffic was modeled as data transmissions from the UEs to the eNB. The arrival of the background data calls followed a Poisson process with average arrival rate λ, and the data call size was randomly sampled from a lognormal distribution with mean M=800 kbits and a coefficient of variation C=1.5. The position of the background call in the cell was selected randomly within the bounds of the LTE cell, and its position did not change throughout the whole transmission (zero mobility assumed for background traffic). Each background data call that arrives in the system enters a buffer (no admission control implemented) and waits there until it is assigned resources from the eNB to start transmitting. When all the data have been sent to the eNB successfully, the entry for the specific data call is erased from the buffer.

As far as the propagation environment is concerned, the shadowing effect and the multipath fading are not modeled, since these propagation effects are dominant in urban environments where there are a lot of reflective surfaces, but for the case of rural environments their effect on the received signal is minimal. Apart from that, the propagation characteristics in our model were calculated as follows. The path-loss of the users in the cell was calculated according to the Okumura-Hata model for rural

areas [7] and from that, the Signal to Interference and Noise Ratio (SINR) per Physical Resource Block (PRB) was calculated according to equation (1):

$$\boldsymbol{SINR^{PRB}} = \frac{\boldsymbol{P_{Tx}^{PRB}/PL}}{\boldsymbol{I+N}} \qquad (1)$$

Where $\boldsymbol{P_{Tx}^{PRB}}$ is the UE transmission power per PRB, $\boldsymbol{PL}$ is the path-loss, $\boldsymbol{I}$ is the interference in Watts and $\boldsymbol{N}$ is the thermal noise in Watts. Since no neighboring cells were modeled to create inter-cell interference, typical values from literature ([8] and [9]) were used, and so the value for interference and thermal noise was set to I = N = -116 dBm.

3 Radio Resource Management

In this section we will discuss how our model allocates the radio resources of LTE (PRBs) to the users of the network. Since the size of the ITS beacons is fixed and known, we have to know the individual bit rate that each user can support at any given moment in order to know and allocate the necessary number of PRBs. In order to do that we used a procedure that models the Adaptive Modulation and Coding scheme (AMC) of LTE, and uses the Shannon bound to calculate the bit rate per PRB for every user. This process is given by equation (2):

$$\boldsymbol{Bit\ Rate^{PRB}} = \boldsymbol{B^{PRB}} \times (\boldsymbol{\alpha} \times \mathbf{log_2}(\mathbf{1} + \boldsymbol{SINR^{PRB}})) \qquad (2)$$

Where B^{PRB} is the band width per PRB (180 kHz) and α is an attenuation factor representing implementation losses. From the literature [7] it was shown that α=0.4 is an appropriate value for the modeling of the UL, while α=0.6 is appropriate for the modeling of the LTE DL. The effect of the highly dynamic vehicular environment and the way it affects the performance of LTE, was taken into account by adjusting the bit rate of each moving vehicle according to its current velocity. This adaptation of the bit rate to the velocity of the vehicles was done according to the findings of LSTI in [10] and the details of implementation in our model are shown below.

- **User velocity**: 1.39 m/s <= v <= 8.35 m/s → **bit rate reduction**: 4%
- **User velocity**: 8.36 m/s <= v <= 33.3 m/s → **bit rate reduction**: 12%
- **User velocity**: 33.3 m/s < v → **bit rate reduction**: 15%

The transmission power used by each user in the LTE network is dictated by the Transmit Power Control (TPC). To avoid the complexity of TPC we chose to implement an open loop power control scheme in our model. In a LTE network, the eNB broadcasts the optimal target received power level per PRB and the UEs choose correspondingly their transmission power levels according to their path loss and the number of PRBs allocated to them at the time. In our model, we assume the users are always aware of the target received power level of the eNB, thus enabling them to calculate their optimal transmission power level in order for their transmission to reach the eNB. The received power level per PRB at the eNB was set at $P_0 = -78$ dBm, based on [8], [9] and [11]. Additionally, we assumed that all vehicles are equipped with the highest class terminals that are defined by the LTE standard. That means that the maximum transmission power of a vehicle is $P_{UE\_MAX} = 23$ dBm, which puts an upper bound to the number of PRBs that can be allocated to the users.

In order to make our model more accurate and realistic a retransmission scheme was implemented to simulate the block error rate of the network. In LTE, packets are retransmitted in case of loss, which affects the transmission time and the available resources significantly. A literature research in [12], [13] and [2] indicated that a retransmission ratio (or packet loss) of 1% for the ITS traffic and 10% for the background traffic was very realistic according to the specifications of the two applications. In our model each time that a retransmission occurs, a retransmission penalty of 8 ms is added to the end-to-end delay of the beacon and the necessary resources for the retransmission are reserved.

As far as resource scheduling is concerned, we chose to implement three different scheduling schemes, dynamic scheduling (fair sharing), dynamic scheduling (priority for ITS traffic) and Semi-Persistent Scheduling (SPS) for ITS traffic/dynamic scheduling for background traffic. When dynamic scheduling is used the eNB makes scheduling decisions and assigns PRBs to the users on demand, every Transmission Time Interval (TTI) which has a duration of 1 millisecond. This process involves a lot of control signaling overhead, since for every beacon, the users have to send requests for resource assignment and the eNB has to signal back to them, with the resource allocation grant. When fair sharing is used, all the users in the network are treated with the same priority, while when priority for ITS traffic is used, the eNB will first serve all the ITS users that have requested resources and if there are remaining resources within this TTI, they will be allocated to the background users.

Semi-Persistent Scheduling (SPS) is a combination of persistent scheduling for initial transmissions and dynamic scheduling for retransmissions. At the beginning of each active period, the UE sends an uplink resource request to the eNB. On receiving the resource request, the eNB allocates a sequence of PRBs located with a certain periodicity between them, where the UE can send all its initial transmissions. When needed, the eNB may reallocate different resources to enable link adaptation. The UE will keep sending its packets using the same PRBs without sending requests or waiting for grants every TTI, until the eNB reallocates the resources of the cell according to the refresh rate of the SPS scheme. In this way a large portion of control signaling is eliminated [13].

The exact gain in resources that is offered by SPS depends on the periodicity and refresh rate that are chosen for the scheme, which in turn depend on the application being served. After some research in [12] and [13] we decided to model our SPS scheme to use 25% of the total control signaling resources that dynamic scheduling is using. The periodicity of the SPS scheme for ITS applications depends on the beaconing frequency of each individual application. The most demanding ITS application have a beaconing frequency of 20 Hz, which means that a SPS periodicity of 50 ms is needed in order to provide resources for the transmission of one beacon every 50 ms. After some testing with our simulator, we came to the conclusion that SPS would operate optimally with a refresh rate of 10 s (persistent allocations are reassigned) and with the assignment of one extra PRB per user in order to accommodate for the highly dynamic vehicular environment which would cause beacons to be dropped because of the outdated PRB allocations.

4 Simulation Results & Analysis

A large number of simulation runs were performed, with different random seeds, in order to ensure statistical accuracy. For all the results that are presented in this paper, the 95% confidence interval is smaller than 4% of the displayed mean value. The values of the main parameters of our model during these simulation runs, are shown in Table I.

Table 1. Simulation parameters values

Parameter	Value	Parameter	Value
N^o of highway lanes	4	Beaconing frequency	10/20 Hz
Road length	2000 m	Beacon size	100 Bytes
LTE Cell radius	1000 m	Average vehicle velocity	30 m/s
Height of eNB	30 m	Velocity fluctuation	6 m/s
No of Background calls	3600	Simulated time	1800 sec
Background call arrival rate	2 calls/sec	Average background call size	800 kbits

As mentioned before, in order for the ITS applications to be able to work over LTE, their beacons have to be delivered within the ITS delay requirements (usually 50 or 100 ms). Figure 2 below depicts the average end-to-end beacon delay experienced by all users in the network for an increasing number of participating vehicles, for two different beaconing frequencies f=10 Hz and f=20 Hz, when dynamic scheduling with fair sharing is used. As we can see, the beacon delay offered by LTE is for

the most part, well below the ITS imposed upper bounds. Under normal load conditions (load below 95%), the beacon delay is around 18 ms and it increases slightly as the load imposed on the network increases.

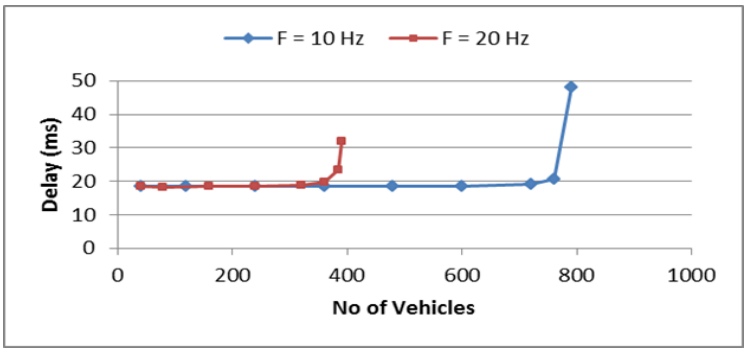

Fig. 2. Average end-to-end beacon delay

Except for the average beacon delay, the cumulative distribution function of the beacon delay for the case of 360 participating vehicles is shown in Figure 3. The figure shows that for both beaconing frequencies, none of the beacons exceeds the most stringent ITS requirement (50 ms) but in the case of f=10 Hz all the beacons are delivered faster due to the decreased load on the network.

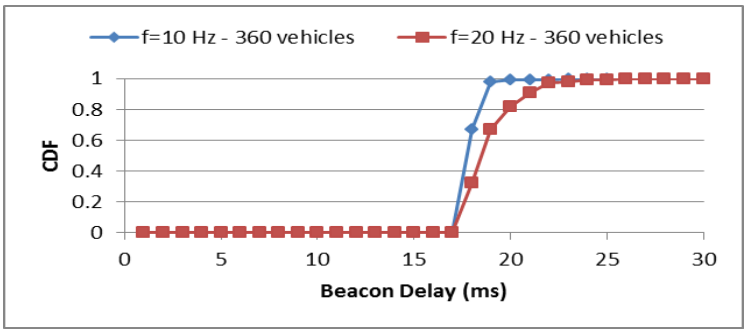

Fig. 3. Cumulative Distribution Function of the end-to-end beacon delay

Another interesting observation is that when the beaconing frequency is doubled the capacity of the LTE network in terms of vehicles that can be served, is almost halved. This is an expected behavior since every vehicle in the network is offering double the load. The fact that none of the beacons experiences a delay lower than 17 ms, even with an unloaded network, is due to the transmission path that every beacon takes through the LTE network. The UL and DL transmission delay, the core network delay, the buffering and processing delay, create this lower limit for the end-to-end beacon delay.

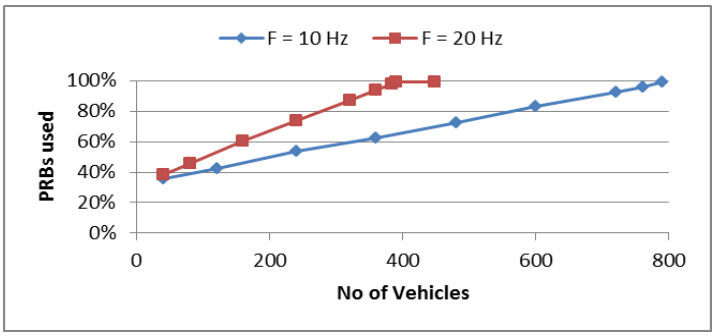

Fig. 4. Total network load vs No of vehicles

Figure 4 shows the percentage of LTE resources (PRBs) used to serve the traffic on the network. As we can see the load increases linearly with the number of vehicles in the network, while the constant background traffic (1.6 Mbps) amounts for about 32% of the load. By comparing this figure with Figure 2 we observe that when the load on the network approaches 100% the beacon delay increases abruptly. The above observations, mean, that LTE can easily serve ITS applications until its capacity limit is reached. As the load of the network gets close to 100%, the performance of LTE degrades abruptly and can no longer serve the ITS applications.

Apart from the performance of ITS applications over LTE we also want to evaluate the effect that the introduction of ITS traffic will have on the existing background LTE traffic. Figure 5 depicts the probability of a background call experiencing throughput below certain thresholds for the case of f=10 Hz and thus giving us an impression about the QoS experienced by the background calls. The figure shows that the throughput of the background calls, drops significantly when the number of vehicles in the network exceeds 600 and the background call QoS is significantly degraded. Even so, a large number of vehicles can be accommodated without having an impact on the performance of the background traffic.

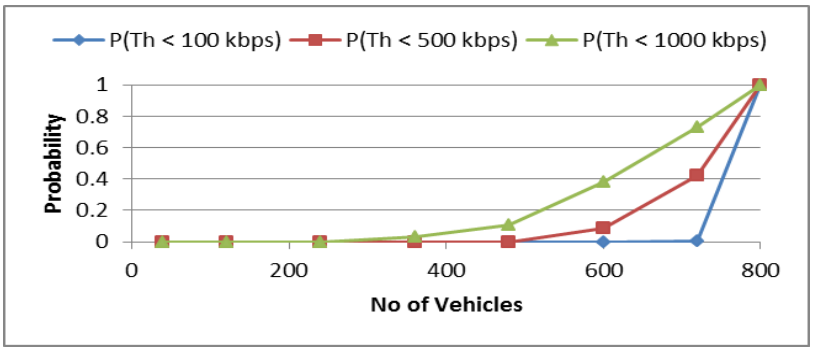

Fig. 5. Probability of a background call experiencing decreased throughput

Figure 6 shows the average end-to-end beacon delay for the different scheduling schemes used for the case of f=20 Hz. Clearly, the performance of the two dynamic schemes is almost identical except for the fact that when priority for ITS is used more vehicles can be accommodated (800 vs 720 for fair sharing), since the vehicles get all of the available PRBs. Of course that means that at the same time, the background traffic is starved and does not get any resources allocated. The performance of SPS is much worse (59 ms) due to the way that this scheme is designed and the unfortunate coincidence that in ITS the beacon generation time and the beacon delivery requirement are the same (50ms). The Semi-Persistent scheduler assigns the resources to the users, keeping in mind that it has to assign enough resources to each vehicle in order to be able to transmit one beacon every 50 ms (beaconing frequency).

The exact timing of the resources assigned to each user is random, the only restriction is, that the time interval from the beacon generation to the time were the user gets its resources, must be, under 50 ms. Unfortunately, that means that most of the time this time interval is around 35 to 40 ms and that only represents the UL buffering time. By adding the rest of the delays that a beacon encounters through the LTE network (UL transmission delay, core network delay, DL transmission delay, etc.) the end-to-end delay of the beacon adds up to around 60 ms.

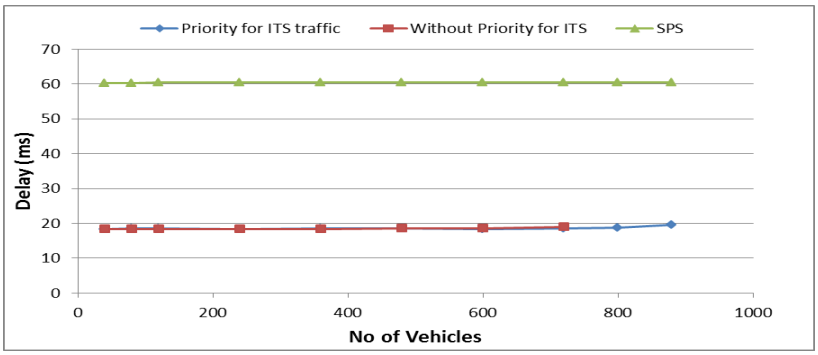

Fig. 6. Average end-to-end beacon delay for different scheduling schemes

On the other hand, SPS saves a lot of system resources compared to the two dynamic schemes, as is shown in Figure 7. As more and more users in the network use SPS (increasing number of vehicles), the less resources are needed for control signaling which means that more resources are available for actual data transmission. When the number of vehicles using SPS is very high compared to the background traffic that uses default dynamic scheduling, as little as 4% of the total system resources are necessary for control signaling. This means that when SPS is used, more users can be accommodated by the network, but the high end-to-end delay of the beacons makes this scheme unsuitable for serving the first class of ITS applications. From the results presented above, we see that LTE can meet the ITS delay requirements for a large number of ITS users (around 600 for f=10 Hz and 300 for f=20 Hz) while at the same time it provides sufficient throughput for the background traffic.

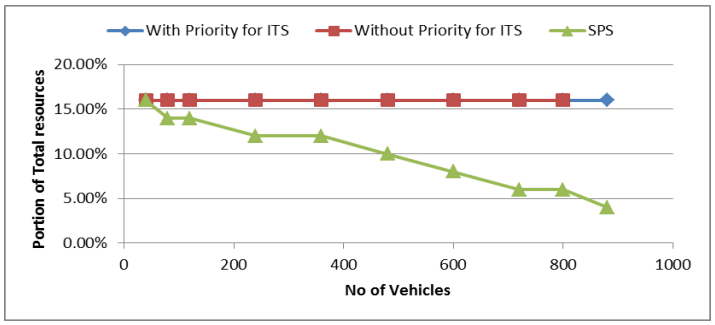

Fig. 7. Resources used for control signaling

In order to compare LTE's performance with that of 802.11p we take into account the work we carried out in [14]. By using the ITS Communication Analyzer (ITSComAn), a simulation tool developed by TNO, we were able to run simulations using 802.11p under similar conditions with those that LTE was tested under and obtain some rough results. The results show that for a network load of 450 vehicles, 802.11p exhibits an extremely low average delay, in the order of 2 ms, while the maximum delay experienced by the vehicles does not surpass 8 ms. Under the same conditions, the average delay offered by LTE is 18 ms (Figure 2).

On the other hand, when using 802.11p a large amount of beacons are lost due to interference, collisions and hidden nodes. At a distance of 50 meters from the transmitter 10% of the beacons are already lost, while at a distance of 600 meters more than 50% of the beacons are lost. Moreover, the transmission range of the vehicles is restricted to 700 meters due to the restriction in the transmission power that they can use. As we have seen in Figures 2 through 5, LTE can accommodate for a larger amount of vehicles (up to 600) with a larger transmission range and without dropping any of the transmitted beacons.

5 Conclusions

From the results presented above, we conclude that LTE can meet most of the requirements of ITS applications, as long as the network's capacity limit has not been reached. When this point is reached the performance of LTE degrades significantly and can no longer meet the ITS requirements. The latencies and capacity offered by LTE under normal network conditions, make it an ideal candidate for use in ITS and at the same time it can accommodate for the background traffic data calls, without compromising the offered QoS beyond certain acceptable limits. The implementation of Semi-Persistent Scheduling in ITS applications can offer some great advantages in terms of capacity of the system, but the fact that the beacon inter-arrival time and the beacon delivery requirement are the same in some ITS applications, make it hard to "harvest" these advantages in ITS implementations.

In comparison with 802.11p, LTE offers larger capacity and larger communication range. On the other hand, 802.11p can offer much lower beacon latencies than LTE,

due to its direct way of communication, in the case that the network is not operating close to its capacity. Moreover, LTE hardly suffers from beacon losses due to collisions, while this is a substantial problem for 802.11p.

In light of the above results we came to the conclusion that a promising solution for communications in a ITS network, would be a combination of the 802.11p and the LTE standards. The 802.11p is more suited to serve the active safety ITS applications, which have stringent delay requirements, because of its extremely low beacon latencies, while LTE is perfectly suited to serve the rest of the ITS traffic thanks to its large capacity. At the same time, since LTE will be handling a large portion of the ITS load, the 802.11p standard will have no scalability or capacity issues.

References

1. 802.11p-2010 - IEEE Standard for Information technology-- Local and metropolitan area networks-- Specific requirements-- Part 11: Wireless LAN MAC and PHY layers Specifications Amendment 6: Wireless Access in Vehicular Environments.
2. ETSI TR 102 638 v1.1.1, Intelligent Transportation Systems (ITS) ; Vehicular Communications ; Basic Set of Applications (BSA); Definitions, ETSI Technical Report, 2009.
3. Konstantinos Trichias, *Modeling and Evaluation of LTE in Intelligent Transportation Systems*, MSc Thesis project, University of Twente, TNO, The Netherlands, 2011.
4. M. Treiber, A. Hennecke and D. Helbing, Microscopic simulation of congested traffic. In: D. Helbing, H. Herrmann, M. Schreckenberg and D. Wolf, Editors, *Traffic and Granular Flow '99*, Springer, Berlin ,2000.
5. Wang Dahui, Wei Ziqiang, and Fan Ying, *Hysteresis phenomena of the intelligent driver model for traffic flow*, Department of Systems Science and Center for Complexity Research, Beijing Normal University, Beijing, China, 2007.
6. Julius Robson, The LTE/SAE Trial Initiative: Taking LTE/SAE from Specification to Rollout, Nortel and LSTI, IEEE Communications Magazine, 2009.
7. Mehdi Amirijoo, Remco Litjens, Ulrich Tuerke, Martin Dottling and Kristina Zetterberg, Cell Outage Management – Models for Cell Outage Copensation", Socrates project internal report, Seventh Framework Programme, TNO.
8. Anas. M; Rosa.C; Calabrese. F.D; Michaelsen. P.H; Pedersen.K.I; Mogensen. P.E, *QoS-Aware Single Cell Admission Control for UTRAN LTE Uplink*, Dept. pf Electronic Systems, Aalborg University, Aalborg, Vehicular Technology Conference, 2008, IEEE.
9. Castellanos, C.U; Villa, D.L; Rosa, C; Pedersen, K.I; Calabrese, F.D; Michaelsen, P.H; Michel, J, *Performance of Uplink Fractional Power Control in UTRAN LTE*, Vehicular Technology Conference, 2008, IEEE.
10. Julius Robson, *Latest Results from the LSTI*, Nortel and LSTI, February 2009.
11. R. Mullner, C. F.Ball, K. Ivanov, J. LienHart, P. Hric, *Performance comparison between open loop and closed loop uplink power control in UTRAN LTE networks*, International conference on Wireless Communications and Mobile Computing, New York, 2009
12. Stefania Sesia, Issam Toufik, Mathew Baker, *LTE, The UMTS Long Term Evolution, From theory to practice*, Wiley editions, 2009.
13. Harri Holma, Antti Toskala, *LTE for UMTS, OFDMA and SC-FDMA Based Radio Access*", Wiley editions, 2009.
14. Konstantinos Trichias, *Statistical Models for Vehicular Communication*, Internship report, TNO and University of Twente, 2011.

Adaptive Energy-Efficient Multi-Tier Location Management in Interworked WLAN and Cellular Network

Yun Won Chung*

School of Electronic Engineering, Soongsil University
511 Sangdo-dong, Dongjak-gu, Seoul, 156-743, Korea

Dual mode mobile stations (MSs), such as smartphone, have been increasingly used recently, and they are generally equipped with WLAN and cellular network interfaces. In dual mode MS with WLAN and cellular network interfaces, mobile users can enjoy high data rate services using WLAN interface and mobility is supported by using cellular interface. Maintaining the two wireless interfaces simultaneously, however, consumes significant battery energy and therefore, an appropriate management of these interfaces has been needed urgently to extend the battery lifetime of an MS.

In [1], [2], works on efficient power management (EPM) were proposed for dual mode MSs with low-tier WLAN and high-tier cellular network interfaces. If an MS does not exchange data using WLAN interface, it turns off the WLAN interface and connectivity with network is maintained using cellular interface, which is turned on always. This is because energy consumption of idle WLAN interface is still significant and it is higher than that of idle cellular interface. If there is any incoming data from WLAN, it is notified through cellular interface and then, WLAN interface is turned on to receive the incoming data. Although this can reduce the energy consumption of dual mode MS significantly, it generates significant paging signaling load, since paging should be performed to all cells within the registered registration area (RA) of cellular network. [3].

For efficient location management of dual mode MSs, single registration (SR) and multi-registration (MR) were proposed [4], where cellular network covers the whole service area but WLAN covers only part of the whole area. In SR, an MS registers at only one available RA at network. However, all available RAs are registered in MR. The tradeoff between SR and MR was analyzed in detail from the aspect of signaling load for location registration and paging. However, energy efficiency was not considered at all, in [4].

In our previous work [5], SR and MR were extended to power efficient SR (PSR) and power efficient MR (PMR) by considering energy efficiency. In PSR, location management is very similar to SR but unregistered wireless interface is turned off. In PMR, location management is very similar to MR. In PMR, if an MS is located within high-tier cellular network only, WLAN interface is turned off. Otherwise, cellular interface is turned off. The performance of SR, MR, PSR,

* This research was supported by Basic Science Research Program through the National Research Foundation of Korea (NRF) funded by the Ministry of Education, Science and Technology (2010-0011464).

PMR, and EPM was analyzed in detail, from the aspect of signaling load and energy consumption, based on mathematical modelling of mobility and traffic characteristics of an MS. From our previous work, it was concluded that PSR and PMR are more energy-efficient than SR and MR, and they have smaller signaling load than EPM. Also, the tradeoff relationship among EPM, PSR, and PMR was observed.

In our future work, we will propose an adaptive energy-efficient multi-tier location management for an MS with WLAN and cellular network interfaces. A cost function is defined as a weighted sum of signaling load and energy consumption to combine two different performance measures. The proposed adaptive management scheme uses measurement-based approach. That is, parameters related with mobility and traffic characteristics of an MS will be measured for a given measurement interval and those for the next interval are estimated using an appropriate estimation approach, such as exponentially weighted moving average. Then, the cost of each scheme is obtained using the estimated parameter values and the scheme with the smallest cost value will be selected for the next interval. Since mobility and traffic characteristics of an MS vary over time, it is essential to select an appropriate measurement interval, which will be determined. Also, the measurement interval should be dynamic to accommodate varying mobility and traffic characteristics efficiently. The proposed scheme is basically per-user basis because mobility and traffic characteristics vary from user to user, and thus, additional signaling overhead for informing the optimal scheme for each user will be introduced, and this will be added to the conventional signaling load. Sensitivity analysis for varying the weights of signaling load and energy consumption will be carried out to give the insight to network operators for network planning. We envision our proposed scheme will achieve the objective of adaptive energy-efficient multi-tier location management efficiently by adapting to varying characteristics of an MS.

References

1. Agarwal, Y., Chandra, R., Wolman, A., Bahl, P., Chin, K., Gupda, R.: Wireless Wakeups Revisited: Energy Management for VoIP over Wi-Fi Smartphones. IEEE MobiSys (2007)
2. Tsao, S. H., Cheng, E. C.: PIANO: a Power Saving Strategy for Cellular/VoWLAN Dual-mode Mobile. Wireless Networks, vol. 14, pp. 683–698. Springer (2008)
3. Chung, Y. W.: Reducing Signaling Load for Power-efficient Integrated WLAN/Cellular Networks. IEICE Electronics Express, vol. 7, no. 9, pp. 652–658. (2010)
4. Lin, Y. B., Chang, L. F. Noerpel, A., Park, K. I.: Performance Modeling of Multi-tier PCS System. International Journal of Wireless Information Networks, vol. 3, no. 2, pp. 67–78. (1996)
5. Chung, Y. W., Lee, S. W.: Modeling and Performance Analysis of Power Efficient Multi-tier Location Management in Interworked WLAN and Cellular Network. Elsevier Mathematical and Computer Modelling, http://dx.doi.org/10.1016/j.mcm.2012.01.007 (2012)

Experimental Analysis of QoS Provisioning for Video Traffic in Heterogeneous Networks

Rossitza Goleva[1], Seferin Mirtchev[1], Dimitar Atamian[1], Desislava Dimitrova[2], Oleg Asenov[3]

[1]Technical University of Sofia, Bulgaria, {rig, stm, dka}@tu-sofia.bg
[2]University of Bern, Switzerland, dimitrova@iam.unibe.ch
[3]St. Cyril and St. Methodius University, Veliko Tarnovo, Bulgaria
olegasenov@abv.bg

Abstract—This work in progress presents video traffic sources specification and analyses at IP layer. The aim is to analyze network segments with video services that tend to congest the channels and find proper configuration parameters in order to avoid overflow. We analyze the Quality of Service (QoS) and Network Performance requirements in wired and wireless LAN as well as 3G network. Measurements and simulations in different network domains help to obtain the presented data. Special attention is paid to networks with video streaming and interactive video services. QoS of heterogeneous sessions is analyzed. The presented ideas are applicable in network design to ensure QoS guarantee and congestion free transmission from user point of view. The study is also relevant to network access and quality management.

Keywords- Multimedia applications*;* Video services; Quality of Service; Bandwidth allocation

1 Video QoS in IP Networks

This paper investigates the Quality of Service (QoS) and Network Performance (NP) requirements of video traffic in IP networks. The necessity of such analyses is based on the network operators' experience of dissatisfactory quality provisioning and irregular congestions in the network segments. Video QoS to DiffServ mapping has been researched extensively last years. Its practical implementation may differ thanks to the traffic mixtures, offered network services, technology constrains. Detailed configuration parameter investigation is still not completed. We investigate how well mapping QoS provisioning to network dimensioning at the IP layer can support the required network performance. The mapping was tested by performing diversity of simulations with various traffic sources for fixed IP and 3G networks. In order to correctly represent traffic sources measurements in wired and wireless LANs and 3G networks were performed and their flow characteristics were analyzed. The analysis of the QoS and NP parameters can help us to determine appropriate ways to map QoS provisioning algorithms, traffic sources, and technology at IP layer in heterogeneous

networks. This will allow application of end-to-end QoS management and more effective and adaptive scheduling.

Based on operator experience it shows that the specific requirements of video applications, e.g., low delays and large number of packets, may cause the (temporal) suppression of other traffic in the network. Therefore, in order to preserve a degree of service fairness, the management of video traffic should be done carefully. Many different approaches in the literature have been proposed to address this problem [1-3]. An idea how to adapt applications to the traffic currently present in the network is shown in [4].

QoS guarantee algorithms like DiffServ, IntServ-RSVP have been a matter of extensive research in the last decade. IntServ-RSVP proved to be better than DiffServ but more expensive. Currently, DiffServ algorithm is the most widely used mechanism on aggregated traffic that has proven to deliver satisfactory performance in practice [5-6]. Furthermore, Pre-Congestion Notification (PCN) and Next Steps in Signaling (NSIS) protocols are designed to guarantee end-to-end QoS [7-8].

A 3G network has defined four types of traffic classes for QoS management. Conversational and streaming classes [9-10] are proper for real-time multimedia applications. However, due to the lack of transparent support by the equipment they are converted into interactive and background classes. In [11] the authors demonstrate a complicated approach towards delay analyses and bandwidth calculation in 802.11e. H.264 video traffic laboratory measurements and simulation in 802.11 with TCP Reno algorithm is shown in [3], [12]. Reported results of delay jitter show that it depends of the assigned priority and is not directly related to the distribution of the inter-arrival time. In practice, network operators compromise by bigger resource provisioning and aggregate traffic prioritization.

The aim of this work is to map configuration management procedures with Quality of Service parameters in wire, wireless and mobile IP environments when the percent of the video traffic is not negligible. The addressed problem has been shown theoretically to exist but it has been rarely monitored in practice. We aim to fill the gap by providing an analysis of real network measurements and using them to argue about system performance. We show that the distribution of the inter-arrival time influences significantly the nature of the traffic.

The paper is organized as follows. First, we study the distributions of the packet sizes and packet inter-arrival times in section 2. Than, we apply these results in simulation models of LAN segment and 3G network. During the simulation, the QoS parameters are conformed and this is the final verification test for the idea presented.

2 Measurements on Video Traffic Sources in Fixed IP Domain and 3G Network

In a fixed IP network, we performed measurements on four traffic types, namely, HTTP transfer, point-to-point (P2P), TV, and VoIP flows. The derived traffic type characteristics are summarized in Table 1. Data traffic collection and analysis is done by Wireshark tool. HTTP measurements we collected in a period of 24 hours for a

worldwide set of queried locations. A typical personal computer is used in all experiments. Queries are performed during peak network hours. The data presented below is the most typical set. The applied browser is Google Chrome. Point-to-Point (P2P) traffic is observed for over 500000 packets in Skype and µtorrent sessions of variable duration. For the TV traffic type, we observed a random channel at iptv.bg for 10 minutes, while for VoIP the traffic generated by Cisco IP Communicator between mobile and IP network was monitored.

From the results in Table 1 we notice that the packet intensity, i.e., the mean number of packets per second, and the session duration vary considerably depending on the type of application. Applications with typically large content transfer such as P2P and TV generate much more packets and have considerably longer sessions than lightweight applications such as HTTP or VoIP. Although this is somewhat expected result its identification is of great importance for QoS provisioning, i.e., the network should be able to provide for the fair treatment of traffic classes with distinct characteristics. Moreover, applications with longer sessions are more vulnerable to fluctuations in the QoS over the different domains of a heterogeneous network.

Table 1. Traffic source observed data in fixed IP network

Parameter	HTTP	P2P	TV	VoIP
Packets intensity, num/sec	50	600	400	60
Mean packet size, bytes	500	800	1000	100
Session duration and mean inter-arrival time (equal)	10 sec	1 hour	1 hour	360 sec
Distribution of session duration and inter-arrival time (equal)	Exponential	Exponential	Exponential	Exponential
Distribution of packets within single burst	Deterministic	Deterministic	Deterministic	Depends on application
Priority of packets	Low	Low	Medium	High

We also measured video traffic in mobile operator's 3G network for two different codecs, namely, H.263 and H.264. Data traffic was measured at the Gi interface in the forward direction on the path between a Node B and a Session Border Gateway Controller (SBC), as shown in Fig. 1. The path passes Radio Network Controller (RNC), Serving GPRS Support Node (SGSN), GGSN Gateway GPRS Support Node (GGSN) and backbone IP transmission network.

The measurements are performed in different busy hour's intervals from different network cells. The traffic at Gi interface is filtered by Wireshark and statistically post-processed. Quality of Service parameters are fully satisfied during the experiments. The observed and analyzed values are typical within the 3G network.

The distribution of packets within a single burst depends mainly on the used codec and the application type. Variable rate codecs generate packets with uniform distribution, while fixed rate codecs generate traffic with uniform or close to exponential distributions. For example, the distribution of packets after Xlite VoIP (codecs such as GSM, G.711) is deterministic whereas the distribution after proprietary Skype codec is closed to uniform [4]. The priority of the service can also change considerably the distribution of the packets after application.

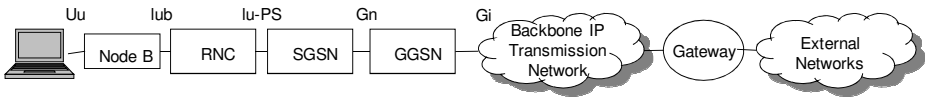

Fig. 1. The observed network architecture

The packet-level traffic characteristics of a single burst in an interactive video session have been studied before by [12-13] and we present them in Table 2. We extend these observations with more detailed analysis of single and multiple bursts.

Fig. 2 shows the packet inter-arrival times and distributions in the forward direction at Gi interface. Single and multiple bursts were considered. Most of the packets sizes are in the range between 180 and 600 bytes and generated with inter-arrival times of up to 20 msec. Differences in inter-arrival time distribution are due to the nature of service and application as well as scheduling.

Table 2. Traffic source specification in 3G network at Gi interface in forward direction

Experiment	Packet size (bytes)	Transport protocol	Inter-arrival time distribution	Packet size distribution
VoIP (GSM 06.01)	100	UDP	Exponential (mean 12 ms)	Deterministic
VoIP (A-law)	230	UDP	Gamma (mean 20 ms)	Deterministic
VoIP (G.729)	80	UDP	Log-normal (mean 12 ms)	Deterministic
VoIP and video (H263)	230	UDP	Exponential (mean 8 ms)	Deterministic
VoIP and video (H264)	230	UDP	Gamma closed to exponential (mean 8 ms)	Deterministic
FTP	40 or 1500	TCP	Gamma (mean 17 ms)	Multi-modal
TV	208	UDP	Almost deterministic	Deterministic

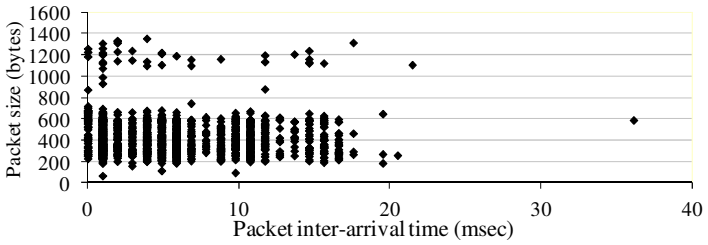

Fig. 2. Packet size versus packet inter-arrival times at Gi interface

Furthermore, the long-range dependence between session duration and number of packets in the session leads to non-trivial distribution of the number of packets versus the inter-arrival time (Fig. 3). Most packets are observed in the time interval of approximately one millisecond. These are packets in the burst when the packets have the same size and deterministic distribution. The second peak on the graph corresponds to inter-arrival times between short bursts in variable rate voice and video streams. The third and fourth peaks correspond to multiple bursts as well but for different session lengths. Our observations are similar to the conclusions drawn from Table 2, i.e., the

distributions of the inter-arrival time within a single on-off traffic source in 3G network tends to be different from typical exponential.

Note that the uplink and downlink traffic characteristics are different and the video traffic in both directions cannot be described with one common model from teletraffic point of view. The packets at the receiving end are shaped based on the scheduling and Quality of Service algorithms applied along by the transmission devices. The shaping effect depends very much on the priority of the packets. Packets with high priority will have less end-to-end queuing delay in comparison to the packets with low priority.

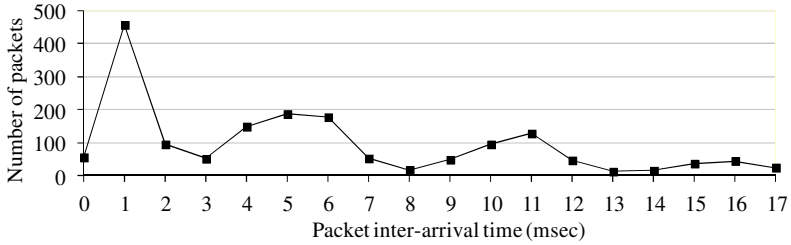

Fig. 3. Number of packets versus packet inter-arrival times at Gi interface for all services

3 Simulations of Video Traffic Sources in Fixed IP Domain and 3G Network

The measurements performed in fixed IP domain were used as input to a simulation model of wired and wireless LANs within the OMNET++ simulator. The observed exponential nature of the burst length allows its straightforward representation in a simulator. The aim is to analyze the fixed IP domain in circumstances not directly verifiable by measurements.

Table 3 shows results for 24 hours simulation. The total number of simulated traffic sources varies between 40 and 200. The number of sources of each service type is equal. Results show that the mean waiting time in a single queue is between 1 and 3 milliseconds, which are acceptable for most end-to-end applications [13]. The high variance of TV and P2P traffic, however, could lead to buffer over dimensioning and resource over provisioning [11]. The long-range dependence of some of the traffic sources, e.g., TV and P2P, is obvious.

In our opinion, traffic separation and partial reservation per traffic type may lead to better performance and QoS guarantee. This can be partially achieved by algorithms such as DiffServ [8] or by enhanced schedulers that dynamically prioritize based on current network load [14]. Given the expected increase in video traffic in wireless networks, however, the latter approach may be quickly incapacitated by the sheer amount of traffic. Therefore, in general, novel approaches towards QoS provisioning in heterogeneous networks may be need. Protocols and QoS mapping in technologies like 4G and DTN where the quality of the signal changes dynamically will require flexible approaches of QoS negotiation.

In similar fashion, we use collected 3G measurements to represent realistic data, voice, and video sources within the ns2 simulator. The simulation model is more complex than the LAN model presented above and covers the entire 3G network as shown in Fig. 1. The TV and the Closed Circuit Television (CCTV) streams are considered asymmetric, whereas the interactive video is considered symmetric. A total of 5, 50, 100, 150, 200 traffic sources are simulated with three priority levels, VoIP having the highest priority and ftp transfer the lowest.

Table 3. Results from simulation in fixed IP domain

Source	Mean rate	Variance	Source	Mean rate	Variance
10 LAN	0,134 Mbps	0,00178 Mbps	50 LAN	6,641 Mbps	0,159 Mbps
10 P2P	0,33 Mbps	1,09 Mbps	50 P2P	15,314 Mbps	50,810 Mbps
10 TV	0,713 Mbps	1,74 Mbps	50 TV	43,479 Mbps	132,882 Mbps
10 VoIP	1.269 Mbps	0.067 Mbps	50 VoIP	1,269 Mbps	0,067 Mbps

The QoS parameters are implemented in Packet Data Protocol (PDP) context and depend on the Home Location Register (HLR). The QoS management at the radio interface is performed in accordance to the 3GPP requirements [15]. The core 3G packet switched network uses DiffServ protocol for QoS management. User data is encapsulated and tunneled in GPRS Tunneling Protocol (GTP) over UDP.

The DiffServ to 3G QoS mapping is different at the radio interface and at the core network [11]. The mapping between IP and 3G network QoS packet marking is done at SGSN for uplink and at GGSN for downlink as well as at HLR. Theoretically, the mapping follows the algorithm shown in the first two columns of Table 4.

Table 4. Theoretical and proposed practical QoS mapping between 3GPP and IETF DiffServ networks

Service	3GPP UMTS QoS class	IETF Diffserv QoS class	3GPP UMTS QoS class	IETF Diffserv QoS class
VoIP	Conversational	EF	Interactive THP=1	VoIP
TV	Streaming	AF21	Interactive THP=3	TV
WWW	Interactive THP=1	AF11	Interactive THP=2	WWW
FTP	Background	BE	Background	FTP

However, the streaming and interactive classes are applied only when they are explicitly specified. Therefore, we propose a mapping as indicated by the last two columns of Table 4, in which there are no conversational and streaming QoS classes. Instead, VoIP and TV traffic types are represented as interactive classes with different priorities. The lower priority of the TV packets adds an additional delay to their transfer times. However, since the TV service is not interactive, we do not expect degradation of the quality perception.

In Table 5 QoS-related data from the performed simulation shows expectedly different parameters for the uplink and downlink, which is strongly influenced by the priority level and scheduling. In the case of packet delay the lower the priority the higher the delay. Hence, we can conclude that QoS can be guaranteed only in case of priorities, traffic shaping, partial bandwidth reservation and over provisioning.

Network dimensioning should take into account traffic mixtures in the network. QoS parameters could change drastically in case of TV flooding or VoIP overloading. Interconnection between mobile and fixed network segments will change the distribution of the traffic and its priority marking. This also can lead to the QoS change.

Simulation results are not directly comparable to measured ones. During measurements, we observed a real network in order to collect information on the behavior of traffic sources, i.e., packet size and inter-arrival time distribution. This information is used in simulation to test the potential network performance for a range of traffic scenarios, which are difficult to realize in a real network. Moreover, in real measurements we are more interested in whether QoS parameters are satisfied. Note that traffic sources are not the same in ns2 and OMNET++ simulation models due to different codecs and specific technology procedures.

Table 5. Video traffic simulation data in 3G network

Parameter	VoIP	TV	WWW	FTP
Packet size (bytes)	208	208	600	1500
Maximal rate (kbps), uplink	80	175	60	50
Maximal rate (kbps), downlink	80	192	125	50
Packet loss, uplink	Up to 2%	Up to 2%	0	0
Packet loss, downlink	Up to 1%	Up to 1%	0	0
Packet delay (ms), uplink	150	100-250	-	-
Packet delay (ms), downlink	80	70-120	-	-
Packet delay jitter (ms), uplink and downlink	2	Less than 3	0	0

Conclusion

This paper discusses first impressions on the QoS support for video traffic in wired and wireless networks. We try to map configuration management algorithms in IP and 3G networks with QoS mechanisms for a range of service classes. The work first presents real measurements of several types of interactive services, e.g., VoIP, streaming, in order to derive traffic characteristics. Different codecs as well as different packet sizes and IP flows are considered. Subsequently, the collected measurements data is used to set simulations such that to investigate the effects of the tested QoS mapping on the end-to-end performance for different traffic mixtures.

We conclude that recent IP cameras require traffic models with rather small packets without fragmentation in order to avoid congestion in the wired and wireless domains, long-range dependence in buffers and heavy-tailed queues. We believe that video traffic should be separated from other types of traffic with bandwidth reservation already at network design. Moreover, the priority level of video streams that tend to flood connections should be carefully chosen. Clear QoS mapping between network domains will improve end-to-end performance. In our future investigations, we will consider mapping QoS requirements at MAC, IP, TCP and application layer as well as QoE evaluation.

Acknowledgements
This paper is sponsored by project “DVU_10_0271 "Public and Private Multimedia Network Throughput Increase by Creating Methods for Assessment, Control, and Traffic Optimization" with National Science Fund, Bulgarian Ministry of Education and Science, 2010 – 2013 leaded by Prof. Ph.D. Vladimir Poulkov.

References

1. Zhang, D., Ionescu, D.: Providing Guaranteed Packet Loss Probability, Service in IP/MPLS-based Networks. In: IEEE ICC 2008 Proceedings, IEEE (2008)
2. Grunwald, D., Sicker, D.: Measuring the Network - Service Level Agreements, Service Level, Monitoring, Network Architecture and Network Neutrality. International Journal of Communication, Vol. 1, 548-566, 1932-8036/20070548 (2007)
3. Haywood, R., Mukherjee S., Peng, X.: Investigation of H.264 Video Streaming over an IEEE 802.11e EDCA Wireless Testbed. In: IEEE ICC 2009 Proceedings, IEEE (2009)
4. Yim, R., Mehta, N., Molisch, A., Zhang, J.: Dual Power Multiple Access with Multipacket Reception Using Local CSI. IEEE Transactions on Wireless Communications, Vol. 8, 4078-4088 (2009)
5. Goleva, R., Goleva, M., Atamian, D., Nikolov, T., Golev, K.: Quality of Service System Approximation in IP Networks. Serdica Journal of Computing, vol. 2, 101-112, ISSN 1312-6555 (2008)
6. Goleva, R., Mirtchev, S.: Traffic Modelling in Disruption-tolerant Networks. In: Annual Seminar of the PTT College “Modelling and Control of Information Processes”, CTP, Sofia, pp. 6-20, ISSN: 1314-2771 (2010)
7. Lehrieder F., Menth, M.: Marking Conversion for Pre-Congestion Notification. In: IEEE ICC 2009 (2009)
8. Good, R., Ventura, N.: End to End Session Based Bearer Control for IP Multimedia Subsystems, Integrated Network Management. In: IM '09 IFIP/IEEE International Symposium on, June 2009, pp. 497 – 504, Long Island, NY, E-ISBN: 978-1-4244-3487-9 (2009)
9. Pradas, D., V´azquez-Castro, M. A.: NUM-Based Fair Rate-Delay Balancing for Layered Video Multicasting over Adaptive Satellite Networks. IEEE Journal on Selected Areas in Communications, Vol. 29, No. 5, 969-978 (2011)
10. Ricciato, F.: Traffic Monitoring and Analyses for the Optimization of a 3G Network. IEEE Wireless Communications, December, 42-49 (2006)
11. Lin, Y., Wong, V.W.S.: Tuning of MIMO-enabled 802.11e WLANs with Network Utility Maximization. In: WCNC 2008 proceedings (2008)
12. Cosma, R., Cabellos-Aparicio, A., Domenech-Benlloch, J., Gimenez-Guzman, J., Martinez-Bauset, J., Cristian, M., Fuentetaja, A., Lopez, A., Domingo-Pascual, J., Quemada, J.: Measurement-Based Analysis of the Performance of Several Wireless Technologies. In: Proceedings of the 16th IEEE Workshop on Local and Metropolitan Area Networks, pp. 19-24 (2008)
13. Spiers, N., Ventura, N.: An Evaluation of Architectures for IMS Based Video Conferencing. Technical Report of University of Cape Town (2008)
14. Dimitrova, D.C., Van den Berg, J.L., Heijenk, G., Litjens, R.: Flow Level Performance Comparison of Packet Scheduling Schemes for EUL UMTS. In: Proceedings of the 6th International Conference on Wired/Wireless Internet Communications, 28-30 May 2008, Tampere, Finland, LNCS 5031 Springer Verlag, pp. 27-40 (2008)
15. 3GPP, TS 23.107 V6.4.0 - Quality of Service (QoS) concept and architecture, [http://www.3gpp.org/ftp/Specs/archive/23_series/23.107/23107-640.zip] (2006)

Author Index